GRI 79/0073

BEHAVIOR OF LNG VAPOR CLOUDS: TESTS TO DEFINE THE SIZE, SHAPE AND STRUCTURE OF LNG VAPOR CLOUDS

ANNUAL REPORT FOR 1979-1980

PREPARED BY

R. N. MERONEY
D. E. NEFF
K. M. KOTHARI

FLUID MECHANICS AND WIND
ENGINEERING PROGRAM
DEPARTMENT OF CIVIL ENGINEERING
COLORADO STATE UNIVERSITY
FORT COLLINS, COLORADO 80523

CONTRACT NO. 5014-352-0203

JULY 1980

Gas Research Institute,
10 West 35th Street,
Chicago, Illinois 60616

GRI 79/0073

BEHAVIOR OF LNG VAPOR CLOUDS: TESTS TO DEFINE THE SIZE, SHAPE AND STRUCTURE OF LNG VAPOR CLOUDS

ANNUAL REPORT FOR 1979-1980

Prepared by

R. N. Meroney
D. E. Neff
K. M. Kothari

Fluid Mechanics and Wind Engineering Program
Department of Civil Engineering
Colorado State University
Fort Collins, Colorado 80523

for

GAS RESEARCH INSTITUTE
Contract No. 5014-352-0203

July 1980

50272-101

REPORT DOCUMENTATION PAGE	1. REPORT NO. GRI 79/0073	2.	3. Recipient's Accession No.
4. Title and Subtitle: The Behavior of LNG Vapor Clouds: Tests to Define the Size, Shape and Structure of LNG Vapor Clouds			5. Report Date: July 1980 6.
7. Author(s): R. N. Meroney, D. E. Neff, and K. M. Kothari			8. Performing Organization Rept. No.
9. Performing Organization Name and Address: Civil Engineering Department, Colorado State University, Fort Collins, Colorado 80523			10. Project/Task/Work Unit No. 5014-352-0203 11. Contract(C) or Grant(G) No. (C) 5014-352-0203 (G)
12. Sponsoring Organization Name and Address: Gas Research Institute, 10 West 35th Street, Chicago, Illinois 60616			13. Type of Report & Period Covered: Interim-Annual 6/1/79-6/30/80 14.

15. Supplementary Notes

16. Abstract (Limit: 200 words)

A terraced 1:240 scale model of the China Lake Naval Weapons Center was constructed to a resolution of one foot vertical increments and placed in the wind tunnel to determine the distances of lower flammability limit (LFL) for 1980, 40 cubic meter spills of Liquefied Natural Gas (LNG) under 4 wind speeds, 5 wind directions, and neutral flow conditions. A set of 8 aspirated hot-wire katharometer probes were made to determine the transient concentration at various downwind locations. Measurements of mean velocities, turbulence intensities, velocity spectra and correlations were performed over the model in the wind tunnel capable of simulating atmospheric phenomena. Data analysis has produced peak concentrations, contours of LFL, and time progressions of the plume ground level LFL. The wind tunnel test should determine the locations of meteorological or concentration instruments set up for field tests. In addition, the expected distances to LFL are determined by wind tunnel tests, thus the field program has the prior knowledge of the distances up to which the measurements should be performed.

17. Document Analysis a. Descriptors

Liquefied Natural Gas, wind tunnel, dispersion of heavy plume

b. Identifiers/Open-Ended Terms

c. COSATI Field/Group

18. Availability Statement	19. Security Class (This Report)	21. No. of Pages 80
	20. Security Class (This Page)	22. Price

(See ANSI-Z39.18) *See Instructions on Reverse*

OPTIONAL FORM 272 (4-77)
(Formerly NTIS-35)
Department of Commerce

GRI DISCLAIMER

LEGAL NOTICE This report was prepared by Colorado State University as an account of work sponsored by the Gas Research Institute (GRI). Neither GRI, members of GRI, not any person acting on behalf of either:

a. makes any warranty or representation, expressed or implied with respect to the accuracy, completeness, or usefulness of the information contained in this report, or that the use of any information, apparatus, method or process disclosed in this report may not infringe privately owned rights; or

b. assumes any liability with respect to the use of, or for damages resulting from the use of, any information, apparatus, method, or process disclosed in this report.

RESEARCH SUMMARY

Title	The Behavior of LNG Vapor Clouds Tests to Define the Size, Shape and Structure of LNG Vapor Clouds GRI Code: GRI 79/0073 GRI Contract Number: 5014-352-0203
Contractor	Civil Engineering Department Colorado State University Fort Collins, Colorado 80523
Principal Investigators	R. N. Meroney, D. E. Neff, and K. M. Kothari
Time Span	July 1979-June 1980 Annual Report
Major Achievements	In a project designed to characterize the behavior of liquefied natural gas (LNG) vapor clouds, wind tunnel tests were conducted during the first year on a terraced 1:240 scale model of the China Lake Naval Weapons Center test site. Measurements of mean wind velocities, turbulent intensities, spectra, and correlations were documented over the Naval Weapons site model. These wind tunnel tests produced data that will determine the best locations to place sensors for actual field tests.
Recommendations	Recommendations were made to Lawrence Livermore Laboratories (test coordinator) for the optimum locations of sensors during the 40 cubic meter LNG spill tests at China Lake, CA.

Description of Work Completed

A 1:240 scale model of the China Lake Naval Weapons Center spill site was constructed. Extensive measurements of wind speed, turbulence, and spectral characteristics of the approach flow were documented. The model was examined in the Environmental Wind Tunnel (EWT) of the Fluid Dynamics and Diffusion Laboratory (FDDL) at Colorado State University. All prefield tests and additional tests at the China Lake Spills were completed. The data analysis for the prefield test series was completed. The scaling law verification tests were performed in the Environmental Wind Tunnel. Correlations of the upwind and lateral plume extent of a simple ground level area source were developed, an improved concentration scaling methodology was devised, and experimental measurements of neutrally buoyant plume dispersion were obtained for ten different wind speed and flow rate combinations. These neutrally buoyant tests were designed to provide a reference scale to the rate of vertical dispersion experienced by plumes of a stable nature.

GRI Comment

This report describes progress on a multitask project. The first task described in this report was carried out to support large scale LNG spill tests at China Lake, California. In the past, instruments were placed at what were believed to be optimal locations by the field test engineers; however, because of terrain and weather vagaries, much of the data was often lost. Using the results of this task, field test engineers were able to situate sensors for maximum data recovery during an LNG spill test. The report also includes analyses and scaling laws that support the use of a wind tunnel to simulate LNG spills. Future work will address the simulation of very large scale spills on land and water and the effects of obstructions on LNG vapor dispersion.

TABLE OF CONTENTS

TABLE OF CONTENTS (continued)

LIST OF FIGURES

LIST OF FIGURES (continued)

LIST OF SYMBOLS

Dimensions are given in terms of mass (m), length (L), time (t), moles (n), and temperature (T).

Symbol	Definition	
A	Area	$[L^2]$
C_p	Specific heat capacity at constant pressure	$[L^2t^{-2}T^{-1}]$
D	Source diameter	[L]
g	Gravitational acceleration	$[Lt^{-2}]$
k	Thermal conductivity	$[mLT^{-1}t^{-3}]$
L	Length	[L]
m	Mass flow rate	$[mt^{-1}]$
M	Molecular weight	$[mn^{-1}]$
n	Mole	[n]
c	Exponent of velocity distributions power law	
p	Pressure	$[mL^{-1}t^{-2}]$
Q	Volumetric rate of gas flow	$[L^3t^{-1}]$
T	Temperature	[T]
ΔT	Temperature difference across some reference layer	[T]
t	Time	[t]
U	Velocity	$[Lt^{-1}]$
$\forall$	Volume	$[L^3]$
W	Plume vertical velocity	$[Lt^{-1}]$
x	General downwind coordinate	[L]
y	General lateral coordinate	[L]
z	General vertical coordinate	[L]
z_o	Surface roughness parameter	[L]
δ	Boundary layer thickness	[L]

LIST OF SYMBOLS (continued)

Symbol	Definition	
Λ	Integral length scale of turbulence	[L]
$\Delta\zeta$	Density difference between source gas and air	$[mL^{-3}]$
ρ	Density	$[mL^{-3}]$
σ	Standard deviation	
χ	Mole fraction of gas component	
Ω	Angular velocity of earth = 0.726×10^{-4} (radians/sec)	$[t^{-1}]$
λ	Wavelength	[L]
ν_o	Eddy viscosity	$[L^2t^{-1}]$

Subscripts

a	Air
Ar	Argon
b.o.	Boiloff
g	Gas
i	Cartesian index
LNG	Liquefied Natural Gas
m	Model
max	Maximum
NG	Natural gas
o	Reference conditions
p	Prototype
r	Reference
s	Source gas

1.0 INTRODUCTION

Natural gas is a highly desirable form of energy for consumption in the United States. Its conversion to heat energy for home and industrial use is achieved with very little environmental impact, and a sophisticated distribution network already services a major part of the country. Recent efforts to expand this nation's natural gas supply include the transport of natural gas in a liquid state from distant gas fields. Unfortunately storage and transport of liquid natural gas may include a relatively large environmental risk (Fay, 1973; Burgess, 1972). To transport and store liquefied natural gas (LNG) it is cooled to a temperature of -162°C. At this temperature if a storage tank on a ship or land were to rupture and the contents spill out onto the earth's surface, rapid boiling of the LNG would ensue and the liberation of a potentially flammable vapor would result. It is envisioned that if the flow from a rupture in a full LNG storage tank could not be constrained 28 million cubic meters of LNG would be released in 80 minutes (AGA, 1974). Past studies (Neff, 1976; AGA, 1974) have demonstrated that the cold LNG vapor plume will remain negatively buoyant for a majority of its lifetime; thus, it represents an extreme ground level hazard. This hazard will extend downwind until the atmosphere has diluted the LNG vapor below the lower flammability limit (a local concentration for methane below 5% by volume).

It is important that accurate predictive models for LNG vapor cloud physics be developed, so that the associated hazards of transportation and storage may be evaluated. Various industrial and governmental agencies have sponsored a combination of analytical, empirical, and physical modeling studies to analyze problems associated with the

transportation and storage of LNG. Since these models require assumptions to permit tractable solution procedure one must perform atmospheric scale tests to verify their accuracy.

A multitask research program has been designed by a combined Gas Research Institute (GRI)/Department of Energy (DOE) effort to address the problem of preditive methods in LNG hazard analysis. One aspect of this program, the physical simulation of LNG vapor dispersion in a meteorological wind tunnel is the subject of this annual progress report. The complete sub-program research contract, GRI contract number 5014-352-0203 consists of three tasks; the first two tasks are data-oriented; whereas the third task is designed to provide documentation and visual presentation of results.

Task 1: Laboratory Support Tests for 1979-80 Forty Cubic Meter Spill Series at China Lake, California.

Task 2: Laboratory Simulation of Idealized Spills on Land/Water; Spill Size 20 to 25,000 m^3.

Task 3: Preparation of Annual and Final Report which Incorporates All Time Results, Background Information, and Confidence Limits.

A more detailed description of these tasks follows.

Task 1: Laboratory Support Tests for 1980 Forty Cubic Meter Spill Series at China Lake, California

The purpose of this study is to provide assistance during field test preparation and basic information on the structure of vapor plumes resulting from LNG spills on land or water for a realistic range of meteorological variables, source variables, and site features. Small-scale models of the LNG Release Pond and surrounding topography at China Lake, Naval Weapons Testing Center, will be placed in a meteorological wind tunnel capable of simulating the appropriate meteorological conditions. Transient concentrations of LNG vapor will be determined by sampling concentrations of tracer gas released from the LNG spill area.

Argon or some other suitable dense gas will be used to simulate the LNG vapor. Overall plume geometry and behavior will be obtained by photographing smoke-tagged effluents.

The general scope of the study includes the following basic elements:

1. Construction of scale models of the LNG Release Pond and surrounding topography at China Lake, California, suitable to simulate various continuous and transient boiloff conditions. The scale chosen will be a compromise between the need to avoid blockage and reflection from wind-tunnel walls and the desire to keep Reynolds number large.

2. Visualization of LNG plume behavior as influenced by various combinations of release rate and meteorological flow conditions.

3. Measurements of transient concentration levels for various combinations of release rate and meteorological flow conditions.

A pre- and post-field test series of measurements will be performed in the laboratory. The first series will help determine the locations of meteorological or concentration instruments such that they intersect dispersing plumes. In addition, any unexpected topographical or dispersive phenomena may be defined in advance of the field test program. The post series of experiments will be utilized to validate laboratory measurements and extend the value of field data.

Pre-field tests have been arranged for 40 cubic spills at 3 spill rates, 4 wind directions, and 3 wind speeds. A summary of the tests proposed are contained in Table 1.

Task 2: Laboratory Simulation of Idealized Spills on Land or Water

The purpose of this study will be to develop an empirical appreciation of the macroscopic physics of LNG vapor transport. Once the dominant mechanisms driving dispersion during the gravity spreading portion of a dense plume moving along a ground plane in a turbulent shear layer are identified, it should be possible to differentiate between the various models proposed by previous investigators. Indeed, as noted in the review Appendices D and F from DOE Report EV-002 (1978), some experts currently assume considerable mixing takes place during gravity spread; whereas others assume no dilution of vapors during this stage of dispersion. It is not surprising then that models based on such a wide variation concerning the kinematics of plume development predict distances to LFL (lower flammability limit) ranging from fractions to tens of miles for the same spill conditions (Haven, 1977).

A series of test model spills are planned to cover the parameter space of dense plume behavior. A cross section of spill volumes, meteorological environments, and boiloff conditions should be examined. These tests will only be performed after a sensitivity analysis has been

performed on existing models to identify test conditions which differentiate between dominant mechanisms or establish functional trends. This approach has previously been successfully applied to warm-plume rise at Colorado State University (Petersen et al., 1978).

As part of such a systematic program designed to identify dense plume dynamics a number of sub-tasks will be accomplished.

a) Since laboratory simulation of LNG spills requires operating wind tunnels at abnormally low wind speeds, a program of measurements will be completed to verify to what extent atmospheric boundary layer similarity actually exists.

b) Investigators are not in agreement as to whether plume entrainment during the gravity spread portion of a dense plume occurs as a result of frontal entrainment or turbulent engulfment as a result of velocity differentials. A small subset of experiments will be planned to evaluate whether the coefficients arising from Lofquist's salt water experiments as utilized by Germeles and Drake (1975), or the mixing process based on the ideas of Cox et al. (1977), or the assumptions of entrainment independent of density gradients proposed by te Riele (1977) are correct for dense gas dilution. Concentration distributions found during steady state release of line-source dense plumes on flat plates and ramps should help differentiate between such concepts.

c) Flammability is dependent on instantaneous local concentrations rather than several minute or hourly averages. Yet current models primarily developed for air pollution evaluation generally give concentrations valid for 3- to 15-minute averaging times. Fast response concentration measurement devices have not been available for field instrumentation during previous test LNG spills. A special effort will be made to produce peak-to-mean statistics from the instantaneous plume behavior during continuous or transient releases.

A summary of tentative tests to be completed in the Colorado State University Environmental Wind Tunnel (EWT) to accomplish the stated objectives is given in Table 2. Additional measurements will be performed as necessary in smaller facilities to identify the entrainment mechanisms.

Task 3: Annual and Final Reports

The annual report will summarize the work performed in the first year. The final report with all experimental results including motion picture film and still photographs of those cases run with material added for visualization, and selected cases of concentration history data on magnetic tape, as well as plots of selected portions of this data will be prepared.

The methods employed in the physical modeling of atmospheric and plume motion are discussed in Chapter 2. The details of model construction and experimental measurements are described in Chapter 3. Chapter 4 discusses the test program and results obtained. Chapter 5 summarizes the conference presentations relating to this investigation. Chapter 6 summarizes the tasks which have been completed. Chapter 7 discusses the work to be performed next year.

2.0 MODELING OF PLUME DISPERSION

To obtain a predictive model for a specific plume dispersion problem one must quantify the pertinent physical variables and parameters into a logical expression that determines their interrelationships. This task is achieved implicitly for processes occurring in the atmospheric boundary layer by the formulation of the equations of conservation of mass, momentum, and energy. These equations with site and source conditions and associated constituitive relations are highly descriptive of the actual physical interrelationship of the various independent (space and time) and dependent (velocity, temperature, pressure, density, etc.) variables.

These generalized conservation statements subjected to the typical boundary conditions of atmospheric flow are too complex to be solved by present analytical or numerical techniques. It is also unlikely that one could create a physical model for which exact similarity exists for all the dependent variables over all the scales of motion present in the atmosphere. Thus, one must resort to various degrees of approximation to obtain a predictive model. At present purely analytical or numerical solutions of plume dispersion are unavailable because of the classical problem of turbulent closure (Hinze, 1975). Such techniques rely heavily upon empirical input from observed or physically modeled data. The combined empirical-analytical-numerical solutions have been combined into several different predictive approaches by Pasquill (1974) and others. The estimates of dispersion by these approaches are often crude; hence, they should only be used when the approach and site terrain are uniform and without obstacles. Boundary layer wind tunnels are capable of physically modeling plume processes in the atmosphere

under certain restrictions. These restrictions are discussed in the next few sections.

2.1 PHYSICAL MODELING OF THE ATMOSPHERIC BOUNDARY LAYER

The atmospheric boundary layer is that portion of the atmosphere extending from ground level to approximately 100 meters within which the major exchanges of mass, momentum, and heat occur. This region of the atmosphere is described mathematically by statements of conservation of mass, momentum, and energy (Cermak, 1971). The general requirements for laboratory-atmospheric-flow similarity may be obtained by fractional analysis of these governing equations (Kline, 1965). This methodology is accomplished by scaling the pertinent dependent and independent variables and then casting the equations into dimensionless form by dividing through by one of the coefficients (the inertial terms in this case). Performing these operations on such dimensional equations yields dimensionless parameters commonly known as:

Reynolds number	$Re = U_o L_o / \nu_o$	$= \frac{\text{Inertial Force}}{\text{Viscous Force}}$
Bulk Richardson number	$Ri = [(\Delta T)_o / T_o] \, (L_o / U_o^2) \, g_o$	$= \frac{\text{Gravitational Force}}{\text{Inertial Force}}$
Rossby number	$Ro = U_o / L_o \Omega_o$	$= \frac{\text{Inertial Force}}{\text{Coriolis Force}}$
Prandtl number	$Pr = \nu_o / (k_o / \rho_o C_{p_o})$	$= \frac{\text{Viscous Diffusivity}}{\text{Thermal Diffusivity}}$
Eckert number	$Ec = U_o^2 / C_{p_o} \, (\Delta \bar{T})_o$	

For exact similarity between different flows which are described by the same set of equations, each of these dimensionless parameters must be equal for both flow systems. In addition to this requirement, there must be similarity between the surface-boundary conditions.

Surface-boundary condition similarity requires equivalence of the following features:

a. Surface-roughness distributions,

b. Topographic relief, and

c. Surface-temperature distribution.

If all the foregoing requirements are met simultaneously, all atmospheric scales of motion ranging from micro to mesoscale could be simulated within the same flow field for a given set of boundary conditions (Cermak, 1975). However, all of the requirements cannot be satisfied simultaneously by existing laboratory facilities; thus, a partial or approximate simulation must be used. This limitation requires that atmospheric simulation for a particular wind-engineering application must be designed to simulate most accurately those scales of motion which are of greatest significance for the given application.

2.1.1 Partial Simulation of the Atmospheric Boundary Layer

A partial simulation is practically realizable only because the kinematics and dynamics of flow systems above a certain minimum Reynolds number are independent of this number's magnitude (Schlichting, 1968; Zoric, 1972). The magnitude of the minimum Reynolds number will depend upon the geometry of the flow system being studied. Halitsky (1969) reported that for concentration measurements on a cube placed in a near uniform flow field the Reynolds number required for invariance of the concentration distribution over the cube surface and downwind must exceed 11,000. Because of this invariance exact similarity of Reynolds parameter is neglected when physically modeling the atmosphere.

When the flow scale being modeled is small enough such that the turning of the mean wind directions with height is unimportant,

similarity of the Rossby number may be relaxed. For the case of dispersion of LNG near the ground level the Coriolis effect on the plume motion would be extremely small.

The Eckert number for air is equivalent to $0.4\ M_a^2\ (\frac{T_o}{\Delta T_o})$ where M_a is the Mach number (Hinze, 1975). For the wind velocities and temperature differences which occur in either the atmosphere or the laboratory flow the Eckert number is very small; thus, the effects of energy dissipation with respect to the convection of energy is negligible for both model and prototype. Eckert number equality is relaxed.

Prandtl number equality is easily obtained since it is dependent on the molecular properties of the working fluid which is air for both model and prototype.

Bulk Richardson number equality may be obtained in special laboratory facilities such as the Meteorological Wind Tunnel at Colorado State University (Plate, 1963).

Quite often during the modeling of a specific flow phenomenon it is sufficient to model only a portion of a boundary layer or a portion of the spectral energy distribution. This relaxation allows more flexibility in the choice of the length scale that is to be used in a model study. When this technique is employed it is common to scale the flow by any combination of the following length scales, δ, the portion of the boundary layer to be simulated; z_o, the aerodynamic roughness; Λ_i, the integral length scale of the velocity fluctuations, or λ_p, the wavelength at which the peak spectral energy is observed.

Unfortunately many of the scaling parameters and characteristic profiles are difficult to obtain in the atmosphere. They are infrequently known for many of the sites to which a model study is to

be performed. To help alleviate this problem Counihan (1975) has summarized measured values of some of these different discriptions for the atmospheric flow at many different sites and flow conditions.

2.2 PHYSICAL MODELING OF PLUME MOTION

In addition to modeling the turbulent structure of the atmosphere in the vicinity of a test site it is necessary to properly scale the plume source conditions. One approach would be to follow the methodology used in Section 2.1, i.e., writing the conservation statements for the combined flow system followed by fractional analysis to find the governing parameters. An alternative approach, the one which will be used here, is that of similitude (Kline, 1965). The method of similitude obtains scaling parameters by reasoning that the mass ratios, force ratios, energy ratios, and property ratios should be equal for both model and prototype. When one considers the dynamics of gaseous plume behavior the following nondimensional parameters of importance are identified (Hoot, 1974; Skinner, 1978; Snyder, 1972; Halitsky, 1969).[1,2]

$$\text{Mass Ratio} = \frac{\text{mass flow of plume}}{\text{effective mass flow of air}}$$

$$= \frac{\rho_s W_s A_s}{\rho_a U_a A_a} = \frac{\rho_s Q}{\rho_a U_a L^2}$$

---

[1] It has been assumed that the dominant transfer mechanism is that of turbulent entrainment. Thus the transfer processes of heat conduction, convection, and radiation are negligible.

[2] The scaling of plume Reynolds number is also a significant parameter. Its effects are invariant over a large range thus making it possible to scale the distribution of mean and turbulent velocities and relax exact parameter equality.

Momentum Ratio $= \dfrac{\text{inertia of plume}}{\text{effective inertia of air}}$

$$= \frac{\rho_s W_s^2 A_s}{\rho_a U_a^2 A_a} = \frac{\rho_s Q^2}{\rho_a U_a^2 L^4}$$

Densimetric Froude No. (Fr) $= \dfrac{\text{effective inertia of air}}{\text{buoyancy of plume}}$

$$= \frac{\rho_a U_a^2 A_a}{g(\rho_g - \rho_a)\forall_s} = \frac{U_a^2}{g\left(\dfrac{\rho_s - \rho_a}{\rho_a}\right)L}$$

Volume Flux Ratio $= \dfrac{\text{Volume flow of plume}}{\text{effective volume flow of air}}$

$$= \frac{Q}{UL^2}$$

To obtain simulataneous simulation of these four parameters it is necessary to maintain equality of the plume's specific gravity ρ_s/ρ_a.

2.2.1 Partial Simulation of Plume Motion

The restriction to an exact variation of the density ratio for the entire life of a plume is difficult to meet for plumes which simultaneously vary in molecular weight and temperature. To emphasize this point more clearly, consider the mixing of two volumes of gas, one being the source gas, $\forall_s$, the other being ambient air, $\forall_a$. Consideration of the conservation of mass and energy for this system yields (Skinner, 1978):[1]

$$\frac{\rho_g}{\rho_a} = \frac{\dfrac{\rho_s}{\rho_a}\forall_s + \forall_s}{\left(\dfrac{T_a}{T_s}\forall_s + \forall_a\right)\left(\dfrac{C_{p_s} M_s}{C_{p_a} M_a}\forall_s + \forall_a\right)\Big/\left(\dfrac{C_{p_s} M_s}{C_{p_a} M_a}\dfrac{T_a}{T_s}\forall_s + V_a\right)}$$

[1]The pertinent assumption in this derivation is that the gases are ideal and properties are constant.

If the temperature of the air, T_a, equals the temperature of the source gases, T_s, or if the product, C_pM, is equal for both source gas and air then the equation reduces to:

$$\frac{\rho_g}{\rho_a} = \frac{\frac{\rho_s}{\rho_a} \forall_s + \forall_a}{\forall_s + \forall_a} \tag{2-8}$$

Thus for two prototype cases: 1) an isothermal plume and 2) a thermal plume which is composed of air, it does not matter how one models the density ratio as long as the initial density ratio value is equal for both model and prototype.

For a plume whose temperature, molecular weight, and specific heat are all different from that of the ambient air, i.e., a cold natural gas plume, equality in the variation of the density ratio upon mixing must be relaxed slightly if one is to model utilizing a gas different from that of the prototype.[1] In most situations this deviation from exact similarity is very small. (See discussion Section 2.3.2 and Figure 2)

Scaling of the effects of heat transfer by conduction, convection, radiation, or latent heat release from entrained water vapor cannot be reproduced when the model source gas and environment are isothermal. Fortunately in a large majority of industrial plumes the effects of heat transfer by conduction, convection, and radiation from the environment are small enough that the plume buoyancy essentially remains unchanged. The influence of latent heat release by moisture upon the plume's buoyancy is a function of the quantity of water vapor present in the

[1] If one was to use a gas whose temperature is different from that of the ambient air then consideration of similarity in the scaling of the energy ratios must be considered.

plume and the humidity of the ambient atmosphere. Such phase change effects on plume buoyancy can be very pronounced in some prototype situations. Figure 1 displays the variation of specific gravity from a spill of liquified natural gas in atmospheres of different humidities.

A reasonably complete simulation may be obtained in some situations even when modified density ratio ρ_s/ρ_a is stipulated. The advantage of such a procedure is demonstrated most clearly by the statement of equality of Froude Numbers.

$$\left(\frac{U_a^2}{(\frac{\rho_s}{\rho_a} - 1)Lg}\right)_m = \left(\frac{U_a^2}{(\frac{\rho_s}{\rho_a} - 1)Lg}\right)_p$$

Solving this equation to find the relationship between model velocity and prototype velocity yields:

$$(U_a)_m = \left(\frac{S.G._m - 1}{S.G._p - 1}\right)^{\frac{1}{2}} \left(\frac{1}{L.S.}\right)^{\frac{1}{2}} (U_a)_p$$

where S.G. is the specific gravity, (ρ_s/ρ_a), and L.S. is the length scale, (L_p/L_m). By increasing the specific gravity of the model gas compared to that of the prototype gas, for a given length scale, one increases the reference velocity used in the model. It is difficult to generate a flow which is similar to that of the atmospheric boundary layer in a wind tunnel run at very low wind speeds. Thus the effect of modifying the models specific gravity extends the range of flow situations which can be modeled accurately. But unfortunately during such adjustment of the model gas's specific gravity at least two of the four similarity parameters listed must be neglected. The options as to which two of these parameters to retain, if any, depends upon the physical situation being modeled. Two of the three possible options are listed below.

(1) Froude No. Equality
Momentum Ratio Equality
Mass Ratio Inequality
Velocity Ratio Inequality[1]

(2) Froude No. Equality
Momentum Ratio Inequality
Mass Ratio Inequality
Velocity Ratio Equality

Both of these schemes have been used to model plume dispersion downwind of an electric power plant complex (Skinner, 1978) and (Meroney, 1974) respectively.

The modeling of the plume Reynolds number is relaxed in all physical model studies. This parameter is thought to be of small importance since the plume's character will be dominated by background atmospheric turbulence soon after its emission. But, if one was interested in plume behavior near the source, then steps should be taken to assure that the model's plume is fully turbulent.

2.3 MODELING OF PLUME DISPERSION AT CHINA LAKE

In the sections above a review of the extent to which wind tunnels can model plume dispersion in the atmospheric boundary layer has been presented. In this section these arguments will be applied to the specific case of an LNG spill at the China Lake Naval Weapons Center.

2.3.1 Physical Modeling of the China Lake Atmospheric Surface Layer

In order to obtain a proper wind tunnel scaling of the China Lake surface layer winds the approach flow characteristics must be similar. To achieve these upstream flow conditions, the wind tunnel must be modified through the introduction of surface roughness elements and

[1]When this technique is employed distortion in velocity scales or similarly volume flow rates requires a correction in source strength.

boundary layer trip devices in such a way that similarity is obtained in both the mean velocity variation with height and the characteristic length scales of turbulence. A convenient parameter which characterizes the mean velocity variation with height is z_o, the aerodynamic roughness height, (Schlichting, 1968) as defined by log-linear description of velocity variation in a boundary layer. A convenient parameter which characterizes the scales of turbulent velocity fluctuations is Λ_i, the integral scale of turbulence (Hinze, 1975).

The conditions in the wind tunnel were adjusted until both of these length scales were in the same proportion to their atmospheric equivalents (obtained from Counihan, 1975) as the geometric length scale chosen for the model's terrain construction. The optimal geometric length scale was 1:240.

2.3.2 Physical Modeling of the China Lake LNG Spill Plume

The buoyancy of a plume resulting from an LNG spill is a function of both the mole fraction of methane and temperature. If the plume entrains air adiabatically, then the plume would remain negatively buoyant for its entire lifetime. If the humidity of the atmosphere were high then the state of buoyancy of the plume will vary from negative to weakly positive. These conclusions are born out in Figure 1, which illustrates the specific gravity of a mixture of methane at boiloff temperature with ambient air and water vapor.

Since the adiabatic plume assumption will yield the most conservative downwind dispersion estimates this situation was simulated. Several investigators have confirmed that the Froude number is the parameter which governs plume spread rate, trajectory, plume size, and

entrainment during initial dense plume dilution (Hoot and Meroney, 1974; Bodurtha, 1961; Van Ulden, 1974; Boyle and Kneebone, 1973). The modeling of momentum is not of critical importance for a ground source released over a fairly large area. The equality of model and prototype specific gravity was relaxed so that pure Argon gas could be used for the model source gas.

Argon provides almost eight times the detection sensitivity for instantaneous concentration measurements as the carbon dioxide used in previous studies (Meroney, 1977). The variation of specific gravity with equivalent observed mole fraction of methane for these different gases is plotted in Figure 2. The variation of Froude number with equivalent mole fraction of methane for the simulation gas used, Argon, is plotted in Figure 3. Over the concentration range where the buoyancy forces are dominant the variation of the Froude number is properly simulated. Undistorted scaling of velocity components was maintained, which implies the undistorted scaling of source strength.

The actual source condition, boiloff rate per unit area over the time duration of the spill, for a spill of LNG on water is highly unpredictable. There was no data on the variable area and variable volume nature of the different LNG tests to be conducted at China Lake thus the source conditions were approximated by assuming a steady boiloff rate for the duration of the spill over a constant area.

Since the thermally variable prototype gas was simulated by an isothermal simulation gas, the concentration measurements observed in the model must be adjusted to equivalent concentrations that would be measured in the field. This relationship which is derived in Appendix A is:

$$\chi_p = \frac{\chi_m}{\chi_m + (1 - \chi_m)\frac{T_s}{T_a}}$$

where

χ_m = volume or mole fraction measured during the model tests,

T_s = source temperature of LNG during field conditions,

T_a = ambient air temperature during field conditions,

and χ_p = volume or mole fraction in the field.

3.0 DATA AQUISITION AND ANALYSIS

The methods used to make laboratory measurements and the techniques used to convert these measured quantities to meaningful field equivalent quantities are discussed in this section. Attention has been drawn to the limitations in the techniques in an attempt to prevent misinterpretation or misunderstanding of the results presented in the next section. Some of the methods used are conventional and need little elaboration.

3.1 WIND TUNNEL FACILITIES

The Environmental Wind Tunnel (EWT) shown in Figure 4 was used for the remaining three test series. This wind tunnel, specially designed to study atmospheric flow phenomena, incorporates special features such as adjustable ceiling, rotating turntables, transparent boundary walls, and a long test section to permit reproduction of micrometeorological behavior at larger scales. Mean wind speeds of 0.15 to 12 m/s can be obtained in the EWT. A boundary layer depth of 1 m thickness at 6 m downstream of the test entrance can be obtained with the use of the vortex generators at the test section entrance and surface roughness on the floor. The flexible test section roof on the EWT is adjustable in height to permit the longitudinal pressure gradient to be set to zero. The vortex generators at the tunnel's entrance were followed by 10 m of smooth floor, and a 3 m approach ramp to the 1:240 scaled topography at the China Lake site.

3.2 MODEL

For reasonable reproduction of the characteristics of the surface winds at China Lake site, a model scale of 1:240 was decided on. The topography of the China Lake terrain was simulated by the construction of a layered model, each layer (0.05 in. tack board) was representative

of a one-foot elevation change at the site. A hole was cut in the center of the spill pool to accomodate the appropriate size area source, and buildings and roads were placed on the model for reference points. Figure 5 is a photograph of the topographic model. The source gas, Argon, stored in a high pressure cylinder was directed through a solenoid valve, a flow meter, and onto the circular area source mounted in the model pond.

3.3 FLOW VISUALIZATION TECHNIQUES

Smoke was used to define plume behavior over the China Lake site. The smoke was produced by passing the simulation gas, Argon, through a container of titanium tetrachloride located outside the wind tunnel. The plume was illuminated with arc-lamp beams. A visible record was obtained by means of pictures taken with a Speed Graphic camera utilizing Polaroid film for immediate examination. Additional still pictures were obtained with a 35 mm camera. The color motion pictures were taken with a Bolex motion picture camera.

3.4 WIND PROFILE AND TURBULENCE MEASUREMENTS

Velocity profile measurements, reference wind speed conditions, and turbulence measurements were obtained with a Thermo-Systems Inc. (TSI) 1050 anemometer and a TSI model 1210 hot film probe. Since the voltage response of these anemometers is non-linear with respect to velocity, a multi-point calibration of system response versus velocity was utilized for data reduction.

The velocity standard utilized in the present study was that depicted in Figure 6. This consisted of a Matheson model 8116-0154 mass flowmeter, a Yellowsprings thermistor, and a profile conditioning section constructed by the Engineering Research Center shop. The mass

flowmeter measures mass flow rate independent of temperature and pressure, the thermistor measures the temperature at the exit conditions, and the profile conditioning section forms a flat velocity profile of very low turbulence at the position where the probe is to be located. Incorporating a measurement of the ambient atmospheric pressure and a profile correction factor permits the calibration of velocity at the measurement station from 0.0-2.0 m/s ±5.0 cm/s.

During calibration of the single film anemometer, the anemometer voltage response values over the velocity range of interest were fit to an expression similar to that of King's law (Sandborn, 1972) but with a variable exponent determined by least squares method. The accuracy of this technique is approximately ±2 percent of the actual longitudinal velocity.

The velocity sensors were mounted on a vertical traverse and positioned over the measurement location on the model. The anemometer's responses were fed to a Preston analog-to-digital converter and then directly to a HP-1000 minicomputer for immediate interpretation. The HP-1000 computer also controls probe position. A flow chart depicting the control sequence for this process is presented in Figure 7.

3.5 CONCENTRATION MEASUREMENTS

To obtain the concentration time histories at points downwind of the spill site a rack of eight hot-wire aspirating probes was designed and constructed. A layout of this design is presented in Figure 8. The films on these probes were replaced with 0.005 in. platinum wire to improve signal-to-noise characteristics. These eight instantaneous concentration sensors were connected to an eight-channel TSI hot-wire anemometer system. The output voltages from the TSI unit are conditioned

for input to the analog-to-digital converter by a DC-supression circuit, a passive low-pass filter circuit tuned to 100 Hz, and an operational amplifier of times five gain. A schedule of this process is shown in Figure 9.

3.5.1 Hot Film Aspirating Probe

The basic principles governing the behavior of aspirating hot wire probes have been discussed by Blackshear and Fingerson (1962), Brown and Rebollo (1972), and Kuretsky (1967). A vacuum source sufficient to choke the flow through the small orifice just downwind of the sensing element was applied. This wire was operated in a constant temperature mode at a temperature above that of the ambient air temperature. A feedback amplifier maintained a constant overheat resistance through adjustment of the heating current. A change in output voltage from this sensor circuit corresponds to a change in heat transfer between the hot-wire and the sampling environment.

The heat transfer rate from a hot-wire to a gas flowing over it depends primarily upon the wire diameter, the temperature difference between the wire and the gas, the thermal conductivity and viscosity of the gas, and the gas velocity. For a wire in an aspirated probe with a sonic throat, the gas velocity can be expressed as a function of the ratio of the probe cross-sectional area at the wire position to the area at the throat, the specific heat ratio, and the speed of sound in the gas. The latter two parameters, as well as the thermal conductivity and viscosity of the gas mentioned earlier, are determined by the gas composition and temperature. Hence, for a fixed probe geometry and wire temperature, the heat transfer rate, or the related voltage drop across the wire is a function of only the gas composition and temperature.

Since all tests performed in this study were in an isothermal flow situation the wire's response was only a function of gas composition.

During probe calibration known compositions of Argon-air mixtures were passed through a pre-heat exchanger to condition the gas to the tunnel temperature environment. These known compositions were produced from a bottle of pure Argon and bottle of pure air passed through a Matheson gas proportioner or drawn from a bottle of prepared gas composition provided by Matheson Laboratories. For an overheat ratio (temperature of wire/ambient temperature) of 1.75 the voltage drop varies approximately linearly with Argon concentration and has the maximum sensitivity. This particular overheat ratio was used during all wind tunnel measurements.

3.5.2 Errors in Concentration Measurement

The effective sampling area of the probe inlet is a function of the probe's aspiration rate and the distribution of approach velocities of the gases to be sampled. A calculation of the effective sampling area during all tests suggests that the effective sampling area was approximately 0.5 cm^2. Thus the resolution of the concentration measurements as applied to the China Lake site is 2.9 m^2.

The travel time from the sensor to the sonic choke limits the upper frequency response of the probe. At high frequencies the correlation between concentration fluctuation and velocity fluctuations (velocity fluctuations are a result of the changes of sonic velocity with concentration) at the sensor begin to decline. The CSU aspirated probe is expected to have a 1000 Hz upper frequency response, but, to improve signal to noise characteristics, the signal was filtered at 100 Hz.

This is well above the frequencies of concentration fluctuations that were expected to occur.

The accumulative error, due to the combined effect of calibration uncertainties and non-linear voltage drifting during the testing time, is estimated to be approximately ±10-15 percent (5%-15% equivalent methane concentrations).

3.6 COMPUTER PROGRAM DEVELOPMENT

The Fluid Dynamics and Diffusion Laboratory at Colorado State University uses an HP 1000 minicomputer system connected to a Preston analog-digital data acquisition system for a majority of experimental measurements. From the Environmental Wind Tunnel (EWT), where all the experimental measurements for the present contract will be made, a maximum of eight data channels can be patched into the computer system for on-line data analysis.

To fulfill this contract computer programs written in Assembly and Fortran IV languages have been developed. These programs are capable of 1) obtaining records of all digital time series from one or more of the available eight data channels, 2) conversion of these digital voltage levels to meaningful physical quantities such as concentration or velocity, 3) reduction of the resultant time series by methods of probabilistic, spectral, or some other type of description to obtain the pertinent characteristic of the signal being analyzed, and 4) plotting of the actual time series or some of its descriptive characteristics such as spectral energy distribution of velocity field.

4.0 TEST PROGRAM RESULTS (1 JUNE 1979 TO 30 JUNE 1980)

During the first quarter a 1:240 scale model of the China Lake Naval Weapons Center spill site was constructed to a vertical resolution of one foot. Extensive measurements of wind speed, turbulence, and spectral characteristics of the approach flow were documented.

During the second quarter the model was examined in the Environmental Wind Tunnel (EWT) of the Fluid Dynamics and Diffusion Laboratory (FDDL) at Colorado State University. All pre-field tests outlined in Table 1: Summary of Tests, China Lake Spills, were completed. Additional test points and replications were made beyond this outline to validate fully all test procedures and the expected ensemble statistics.

During the third quarter the data analysis for the pre-field test series was completed, scaling law verification tests were performed in the Environmental Wind Tunnel.

During the fourth quarter two different conference presentations of the physical simulation of LNG dispersion were presented and the experimental data acquisition and analysis of scaling law verification tests were continued. Correlations of the upwind and lateral plume extent of a simple ground level area source were developed, an improved concentration scaling methodology was developed, and experimental measurements of neutrally buoyant plume dispersion were obtained for ten different wind speed and flow rate combinations. These neutrally buoyant tests were designed to provide a reference scale to the rate of vertical dispersion experienced by plumes of a stable nature.

4.1 MEAN WIND FIELD SIMULATED OVER CHINA LAKE

The topographic model replicating the China Lake site at a scale of 1:240 was placed in the EWT. The test matrix performed on the model was designed to find the proper upstream tunnel conditions for the correct simulation of the wind fields expected at China Lake. This matrix consisted of measurements of mean velocity profiles (mean velocity variation with elevation) at several locations along the lateral and longitudinal axis of the wind tunnel for different floor roughness configurations, tunnel entrance conditions, and tunnel wind speeds.

The results of this test series indicated that eight tapered spires situated in the tunnel entrance section and a two brick high trip on the tunnel floor were necessary to accelerate the proper development of the desired boundary layer characteristics. The tunnel floor upwind of the model was covered with an open cardboard corrugation which produces a physical height variation of approximately three millimeters.

An example of the variation of wind mean velocity profiles at locations upwind, over, and downwind of the China Lake model is presented in Figure 10. Figure 11 shows the variation of local turbulent intensity at these same measurement points.

It is common to describe empirically the atmospheric winds mean velocity profile for different site conditions by both the log-linear law and the power law. The log-linear law is expressed as:

$$\frac{\bar{U}}{U_*} = \frac{1}{k} \log_e \frac{z-d}{z_o} \quad ,$$

where $\bar{U}$ = mean longitudinal wind speed at height z,

U_* = frictional velocity

k = von Karman's constant $\cong 0.4$,

d = displacement height, and

z_o = roughness length.

A regression on this equation to fit the profile PG4005 yielded z_o = 0.043 meters and U_* = 0.39 meters/sec (the displacement height, d, was forced to equal zero). This value of z_o = 0.043 meters compared favorably with values sited by Counihan (1975) for sites that have similar conditions as those of China Lake.

The power law representation is expressed as,

$$\bar{U} = Az^c$$

where A = fitting parameter

c = power law index.

A regression of this equation to fit the profile PG4005 yielded c = 0.18 and A = 3.4. This value of c = 0.18 compares also with values sited by Counihan (1975).

4.2 ANALYSIS OF CONCENTRATION DATA

For each of the pre-field tests described in Table 1, at least 3 replications of the concentration time histories at 98 different spatial points were obtained. The data acquisition was performed online to a Preston Analog-to-Digital Converter controlled by a Hewlett-Packard 1000 Mini-Computer System. Eight channels of data from eight different concentration sensitive probes were digitized and analyzed simultaneously by the computer system. A printed record of pertinent model information and on-line data verification was provided by a controller at the wind tunnel site. A digitized record of concentration time histories was recorded onto the system disk and later transferred over to digital magnetic tape.

Once the experimental data acquisition was complete, the files were transferred back onto the computer for detailed data analysis. This analysis entailed the plotting of the recorded concentration time

histories on a Tektronic pen plotter and the retrieval of pertinent values such as peak concentration, times of 5 percent arrival, 15 percent arrival, 15 percent end, 5 percent end, and the integral of concentration versus time (dosage).

An example of the plotting of concentration versus time is shown in Figure 12 for three different ground level points downwind of run No. 3 as described in Table 1. Note that the three record replication of the same conditions are plotted together on each graph. From the print out of pertinent values, different types of graphical presentations have been prepared. First, ground level contour plots of peak concentration (see Figure 13-1 to 13-9); second, plots of the maximum limits of flammable zone as a function of distance and time (see Figures 14-1 to 14-5); third, vertical peak concentration profiles at several plume centerline distances downwind (see Figure 15); and fourth time progression of the plume's ground level LFL (see Figures 16-1 16-9). A complete set of the pre-field test series results were also forwarded to the Lawrence Livermore Laboratory for guidance field managements. These results included presentations of (1) computer printouts of pertinent values such as peak concentration, times of 5 percent arrival, 15 percent end, and 5 percent end, and dosage for runs 1-9 in Table 1, (2) concentration versus time plots for each spatial point measured in run No. 3, (3) ground level contour plots of peak concentration for runs 1-9, (4) plots of the maximum limits of the flammable zone as a function of distance and time for runs 1-9, (5) vertical peak concentration profiles at several plume centerline distances downwind for run No. 7, and (6) time progressions of the plume's ground level LFL.

4.3 SCALING PARAMETER TESTS

These tests were designed to improve the understanding of model scaling procedures, determine which scaling parameters are sufficient to insure proper similarity in the resultant concentration field, gain insight to the sensitivity to which variation of these parameters from equality has on the resultant concentration, and to determine what range of field variables can be modeled accurately in the Environmental Wind Tunnel facility. In past and present studies being performed by the Fluid Dynamics and Diffusion Laboratory at Colorado State University the following scaling parameter equality has been maintained.

(1) Geometric Scaling

$L_p/L_m \equiv$ modeling length scale = L.S.

(2) Approach Flow Scaling

$(z_o)_p/(z_o)_m \equiv$ roughness length ratio $\tilde{\approx}$ L.S.

$\Lambda_p/\Lambda_m \equiv$ longitudinal integral scale ratio $\tilde{\approx}$ L.S.

$(c)_p/(c)_m \equiv$ mean velocity power law index ratio $\tilde{\approx}$ 1.

(3) Plume Scaling

$$\text{Froude No.} = \left(\frac{U^2}{(\Delta\rho/\rho)gL}\right)_m = \left(\frac{U^2}{(\Delta\rho/\rho)gL}\right)_p$$

$$\text{Volume Flow Ratio} = \left(\frac{Q}{UL^2}\right)_m = \left(\frac{Q}{UL^2}\right)_p$$

$$\text{Density Ratio} = \left[\frac{\Delta\rho}{\rho}\right]_m \tilde{\approx} \left[\frac{\Delta\rho}{\rho}\right]_p .$$

If some lassitude in exact equality in some of the above scaling parameters does not seriously affect the concentration distribution, then the range of atmospheric variables defining a release scenario may be increased substantially. For example, if the characteristics of the

background turbulence in the approach flow were found to have a small effect on the near field dispersion for a heavy plume, then the approach flow scaling criteria might be relaxed. This would permit scaling of the plume over a larger length scale range than that which is fixed by the wind tunnel capability of scaling the atmosphere. Similarly, if equality in the density ratio is relaxed, then, through the use of a model gas that has a much higher specific gravity than that of methane at boiloff temperatures, it is possible to extend the lower end of the range of atmospheric wind speeds which can be modeled.

4.4 NEAR FIELD GROUND LEVEL BEHAVIOR

A series of visualization tests as described by the run conditions summarized in Table 3 were performed in the Environmental Wind Tunnel (EWT). These tests, performed on a simple ground level area source, covered a range of test variables (wind speed, release rate, source gas specific gravity) in which the plume's upwind spread, L_u, and lateral spread, L_H, away from the source area varied from negligible to many times the diameter of the source. The extent of this upwind and lateral spread for each of these tests were recorded.

Upon analysis of the data it was found that the buoyancy length scale $\ell_b = \frac{Qg\Delta\rho/\rho_a}{U^3}$, was the single parameter to which a satisfactory correlation between test variables and test results was obtained. Britter in an unpublished draft reported a similar result for the spread of saline solutions of varying specific gravities in a fresh water turbulent boundary layer. The correlation of these experimental results are displayed in Figures 17 and 18 where the axis have been non-dimensionalized with respect to the source diameter, D. The parameter ℓ_b/D has the further significance of being the inverse of the Flux

Froude number, $\dot{F}r$, which is derived on an integral approach by Skinner et al., (1978) to be the ratio of the horizontal momentum flux to the plumes buoyancy flux with the Boussinesq approximation. The validity of using the Boussinesq approximation, i.e., that $\rho_{source} \tilde{\approx} \rho_{air}$ in the inertial terms, near the source when $\rho_{source}/\rho_{air} > 1$ is a topic of debate. This question was addressed by comparison of the correlation of the test results with both ℓ_b based on ρ_{air} and ℓ_b based on ρ_{source}. Unfortunately, the experimental error in estimating ℓ_b overshadows any differences between correlations.

From Figures 17 and 18 it is seen that near source lateral and upwind spreading can be expected for values of the Flux Froude number $(U^3D/(Qg(\Delta\rho/\rho_a)))$ of less than 50. The extent of this spreading may be approximated by calculation of this single parameter.

5.0 CONFERENCE PRESENTATIONS

In October of 1979 Dr. Meroney presented a paper entitled "Physical Modeling of Atmospheric Dispersion of Heavy Gases Released at the Ground or From Short Stacks," at the 10th International Technical Meeting on Air Pollution Modeling and Its Application, 23-26 October 1979, Rome, Italy. The presentation was part of a session devoted to heavy gases. The program was devoted to the hazards and dispersion physics of heavy gases such as LNG, Chlorine, and Freon®. The recent series of field releases at Porton Down, England were described together with plans for larger releases in the near future.

We hosted the GRI-LNG Advisory Group on March 18-19, 1980. During the two day period in which the Advisory Group was here we provided a tour of Colorado State University's laboratory facilities, demonstrating the visual appearance of LNG spills over a model of Greenpoint Energy Center of Brooklyn Union Gas Company, and reviewed the pre-test series accomplishments for the China Lake Tests.

During April of 1980 Dr. Meroney was invited to present a short discussion on physical simulation of heavy plume dispersion at the 6th LNG Conference in Kyoto, Japan. This presentation was to the Workshop on Safe Operation of Large Storage Installations held as part of the International Conference and Exhibition on Liquefied Natural Gas. Other presentations considered tank construction and field spills at China Lake, California.

On 18-20 June 1980 Dr. Meroney attended the 4th Colloquium on Industrial Aerodynamics, Aachen, West Germany. A paper entitled "Dispersion of Vapor from LNG Spills - Simulation in a Meteorological Wind Tunnel: Six Cubic Meter China Lake Spill Series," was prepared

together with Mr. David E. Neff. This paper was simultaneously submitted to the Journal of Industrial Aerodynamics for review.

During the rest of 1980, Dr. Meroney will be on sabbatical at the Institute Wasserbau III, University of Karlsruhe, West Germany. During his absence Dr. Kiran Kothari will manage the contract at Colorado State University.

6.0 CONCLUSIONS

A terraced 1:240 scale model of the China Lake Naval Weapons Center was constructed to a resolution of one foot vertical measurements and placed in the wind tunnel to determine the distances of lower flammability limit (LFL) for 1980, 40 cubic meter spill of Liquid Natural Gas (LNG) under 4 wind speeds, 5 wind directions, and neutral flow conditions. The wind tunnel tests should determine the locations of meteorological or concentration instruments set up for field tests so that they intersect the dispersing LNG plume. In addition, the expected distances to LFL are determined in the wind tunnel, thus the field program has prior knowledge of the distances up to which the measurements will be performed.

7.0 WORK PLANNED FOR NEXT YEAR

A wind tunnel test period has been scheduled for early November 1979 in the Environmental Wind Tunnel, Colorado State University, to accomplish all post-test spill configurations as noted on Table 1. All data will be recorded on magnetic tape. Eight simultaneously samples with katharometer probes will be recorded for each run. Each spill will be replicated three to five times. Final data will be reduced to a series of concentration versus time charts as well as information on arrival time, peak concentrations, and departure times. The concentration data with relaxing the plume density will be analyzed.

As indicated on the GANTT chart, Table 4, the test program is essentially on schedule with a number of tasks already completed. The sensitivity analysis of models projected for the first period in Task 2 was delayed to permit early completion of the multi-probe instrumentation in Task 1.

REFERENCES

American Gas Association (1974) "LNG Safety Program, Interim Report on Phase II Work," Report on American Gas Association Project IS-3-1, Battelle Columbus Laboratories.

Blackshear, P. L., Jr., and Fingerson, L. (1962) "Rapid Response Heat Flux Probe for High Temperature Gases," ARS Journal, November 1962, pp. 1709-1715.

Bodurtha, F. T., Jr. (1961) "The Behavior of Dense Stack Gases," J. of APCA, Vol. 11, No. 9, pp. 431-437.

Boyle, G. J. and Kneebone, A. (1973) "Laboratory Investigation into the Characteristics of LNG Spills on Water, Evaporation, Spreading and Vapor Dispersion," Shell Research, Ltd., Report to API, March.

Brown, G. L. and Rebollo, M. R. (1972) "A Small, Fast Response Probe to Measure Composition of a Binery Gas Mixture," AIAA Journal, Vol. 10, No. 5, pp. 649-752.

Burgess, D. S., Biardi, J., and Murphy, J. N. (1972) "Hazards of Spillage of LNG into Water," Bureau of Mines, MIPR No. Z-70099-9-12395.

Cermak, J. E. (1971) "Laboratory Simulation of the Atmospheric Boundary Layer," AIAA Jl., Vol. 9, No. 9, pp. 1746-1754, September.

Cermak, J. E. (1975) "Applications of Fluid Mechanics to Wind Engineering, A Freeman Scholar Lecture," J. of Fluid Engineering, Vol. 97, Ser. 1, No. 1, pp. 9-38.

Counihan, J. (1975) "Adiabatic Atmospheric Boundary Layers: A Review and Analysis of Data from the Period 1880-1972," Atmospheric Environment, Vol. 9, pp. 871-905.

Cox, R. A. and Roe, D. R. (1977) "A Model of the Dispersion of Dense Vapour Clouds," 2nd Intl. Loss Prevention Symposium, Heidelberg, 8 p.

Department of Energy (DOE) (1978) An Approach to Liquified Natural Gas (LNG) Safety and Environmental Control Research, U.S. Department of Energy, Division of Environmental Control Technology, DOE/EV-0002, 446 p.

Fay, J. A. (1973) "Unusual Fire Hazard of LNG Tanker Spills," Combustion Science and Technology, Vol. 7, pp. 47-49.

Germeles, A. E. and Drake, E. M. (1975) "Gravity Spreading and Atmospheric Dispersion of LNG Vapor Clouds," Proceedings 4th Intl. Symposium on Transport of Hazardous Cargoes by Sea and Inland Waterways, Jacksonville, Florida, October 1975, pp. 519-539.

Halitsky, J. (1969) "Validation of Scaling Procedures for Wind Tunnel Model Testing of Diffusion Near Buildings," Geophysical Sciences Laboratory, Report No. TR-69-8, New York University, New York.

Havens, J. A. (1977) "Predictability of LNG Vapor Dispersion from Catastrophic Spills onto Water: An Assessment," Department of Transportation Report, 140 p.

Hinze, J. O. (1975) Turbulence, McGraw-Hill, 790 p.

Kline, S. J. (1965) Similitude and Approximation Theory, McGraw-Hill, 229 p.

Kuretsky, W. H. (1967) "On the Use of an Aspirating Hot-Film Anemometer for the Instantaneous Measurement of Temperature," Thesis, Master of Mechanical Engineering, University of Minnesota, Minneapolis, Minnesota.

Meroney, R. N., et al. (1974) "Wind Tunnel Study of Stack Gas Dispersal at the Avon Lake Power Plant," Fluid Dynamics and Diffusion Laboratory Report CER73-74RNM-JEC-BTY-SKN35, Colorado State University, Fort Collins, Colorado, April.

Meroney, R. N., Neff, D. E., Cermak, J. E., and Megahed, M. (1977) "Dispersion of Vapor from LNG Spills - Simulation in a Meteorological Wind Tunnel," Report prepared for R & D Associates, California, Fluid Dynamics and Diffusion Laboratory Report CER76-77RNM-JEC-DEN-MM57, Colorado State University, Fort Collins, Colorado, 151 p.

Neff, D. E., Meroney, R. N., and Cermak, J. E. (1976) "Wind Tunnel Study of Negatively Buoyant Plume Due to an LNG Spill," Report prepared for R & D Associates, California, Fluid Dynamics and Diffusion Laboratory Report CER76-77DEN-RNM-JEC22, Colorado State University, Fort Collins, Colorado, 241 p.

Pasquill, F. (1974) Atmospheric Diffusion, D. von Nostrand Co., 429 p.

Petersen, R. L., Cermak, J. E., and Meroney, R. N. (1978) "Plume Rise and Dispersion - Effects of Exit Velocity and Atmospheric Stability," Colorado State University Report CER76-77-RLP-JEC-RNM59, 94 p.

Plate, E. J. and Cermak, J. E. (1963) "Micro-Meteorological Wind-Tunnel Facility: Description and Characteristics," Fluid Dynamics and Diffusion Laboratory Report CER63-ELP-JEC9, Colorado State University, Fort Collins, Colorado.

Sandborn, V. A. (1972) Resistance Temperature Transducers, Metrology Press, 545 p.

Schlichting, H. (1968) Boundary Layer Theory, McGraw-Hill, New York.

Skinner, G. T. and Ludwig, G. R. (1978) "Physical Modeling of Dispersion in the Atmospheric Boundary Layer," Calspan Advanced Technology Center, Calspan Report No. 201, May.

Snyder, W. H. (1972) "Similarity Criteria for the Application of Fluid Models to the Study of Air Pollution Meteorology," Boundary Layer Meteorology, Vol. 3, No. 1, September.

te Riele, P. H. M. (1977) "Atmospheric Dispersion of Heavy Gases Emitted at or Near Ground Level," Proceedings of 2nd Intl. Symposium on Loss Prevention and Safety Promotion in the Process Industries, Heidelberg, 6-9 September 1977, pp. 347-357.

van Ulden, A. P. (1974) "On the Spreading of a Heavy Gas Released Near the Ground," Loss Prevention and Safety Promotion Seminar, Delft, Netherlands, 6 p.

Zoric, D. and Sandborn, V. A. (1972) "Similarity of Large Reynolds Number Boundary Layers," Boundary-Layer Meteorology, Vol. 2, No. 3, March, pp. 326-333.

Table 1. Summary of Tests: China Lake Spills

Test Number	Spill Configuration	Wind Speed (m/sec)	Spill Size (m^3)	Spill Rate (m^3/min)	Angles	Concentration Runs (8 Points Each)
Pre-field Test Series						
1	Water	3	40	15	SW	42
2	Water	3	40	30	SW	42
3	Water	5	40	15	SW	42
4	Water	5	40	30	SW	42
5	Water	5	40	30	SW-30°	42
6	Water	5	40	30	SW+30°	42
7	Water	5	40	30	SW+60°	42
8	Water	7	40	15	SW	42
9	Water	7	40	30	SW	42
10	Water	4.9	4.2	4.75	224°	42
Post-field Test Series						
1	Water	(Chosen to				10
2	Water	simulate specific				10
3	Water	field measurement				10
4	Water	conditions)				10
5	Water					
6	Water					

Table 2. Summary of Tentative Tests: Idealized Spills

Test Number	Spill Configuration	Spill Size (m^3)	Scale Ratio	Wind Speed (m/sec)	Stability Category	Concentration Runs (8 points each)	Visualization Cases	Total Test Days
1	Area source water	20	1:200	3	D	10	1	2
2	"	40	1:200	3	D	10	1	2
3	"	100	1:200	3	D	10	1	2
4	"	1,000	1:400	3	D	10	1	2
5	"	10,000	1:400	5	D	10	1	2
6	"	20,000	1:800	5	D	10	1	2
7	Area source land	20	1:200	3	D	10	1	2
8	"	40	1:200	3	D	10	1	2
9	"	100	1:200	3	D	10	1	2
10	"	1,000	1:400	3	D	10	1	2
11	"	10,000	1:400	5	D	10	1	2
12	"	20,000	1:800	5	D	10	1	2
13	Area source land	1,000	1:400	5	D	10	1	2
14	"	1,000	1:400	7	D	10	1	2
15	"	1,000	1:400	3	F	10	1	3
16	"	1,000	1:400	5	F	10	1	3
17	Area source water	1,000	1:400	5	D	10	1	2
18	"	1,000	1:400	7	D	10	1	2
19	"	1,000	1:400	3	F	10	1	3
20	"	1,000	1:400	5	F	10	1	3
					5 weeks in EWT 2 weeks in MWT			44 days

Table 3. Near Field Plume Extent Tests

RUN NO.	SOURCE DIAMETER (cm)	SOURCE GAS SPECIFIC GRAVITY	PLUME DURATION (sec)	FLOW RATE (ccs)	VELOCITY (cm/s)	VELOCITY REFERENCE HEIGHT (cm)	BOUYANCY LENGTH SCALE ℓ_b (cm)	L_u (cm)	L_{H_O} (cm)
1	15	1.38	steady	83	45	1.6	0.3	7.5	15
2	"	"	"	323	56	"	1.4	10	30
3	"	"	"	85	37	"	0.7	8	20
4	"	"	"	647	47	"	2.3	15	36
5	"	"	"	330	37	"	2.5	18	56
6	"	"	"	72	27	"	1.4	10	20
7	"	"	"	43	22	"	1.5	10	36
8	"	"	"	65	22	"	2.3	15	40
9	"	"	"	43	19	"	2.3	15	50
10	"	"	"	280	27	"	5.2	25	92
11	"	"	"	662	37	"	5.2	20	92
12	"	"	"	107	22	"	3.8	18	92
13	"	"	"	419	27	"	7.9	20	102
14	"	"	"	65	18	"	4.1	25	76
15	"	"	"	107	18	"	6.9	33	96
16	"	"	"	699	27	"	13.3	30	122
17	"	"	"	413	22	"	14.5	36	102
18	"	"	"	413	18	"	26.5	66	244
19	"	2.59	"	80	45	"	1.4	7.5+	20
20	"	"	"	160	45	"	2.7	18	50
21	"	"	"	85	37.5	"	2.7	18	60
22	"	"	"	123	37.5	"	4.1	18	60
23	"	"	"	240	45	"	4.1	23	72
24	"	"	"	205	38	"	5.8	25	82
25	"	"	"	86	27	"	6.9	18	60
26	"	"	"	173	27	"	13.7	30	112
27	"	"	"	102	19	"	23.3	46	122
28	"	"	"	153	18	"	41.2	56	152
29	"	"	"	205	18	"	54.9	64	182
30	"	"	"	256	18	"	68.6	69	244
31	"	4.18	"	40	46	"	1.3	10	30
32	"	"	"	80	46	"	2.6	15	46
33	"	"	"	61	38	"	3.5	15	46
34	"	"	"	120	46	"	3.9	18	50
35	"	"	"	197	38	"	11.2	36	122
36	"	"	"	386	47	"	11.6	36	122
37	"	"	"	43	28	"	6.1	13	50
38	"	"	"	396	38	"	22.6	46	152
39	"	"	"	87	28	"	12.3	25	100
40	"	"	"	51	18	"	27.4	33	122
41	"	"	"	334	27	"	53.0	66	200
42	"	"	"	51	16	"	40.0	43	132
43	"	"	"	77	18	"	41.2	48	132
44	"	"	"	500	27	"	80.0	107	244
45	"	"	"	102	18	"	54.9	61	182
46	"	"	"	128	17	"	81.4	76	244

Table 4. GANTT Chart

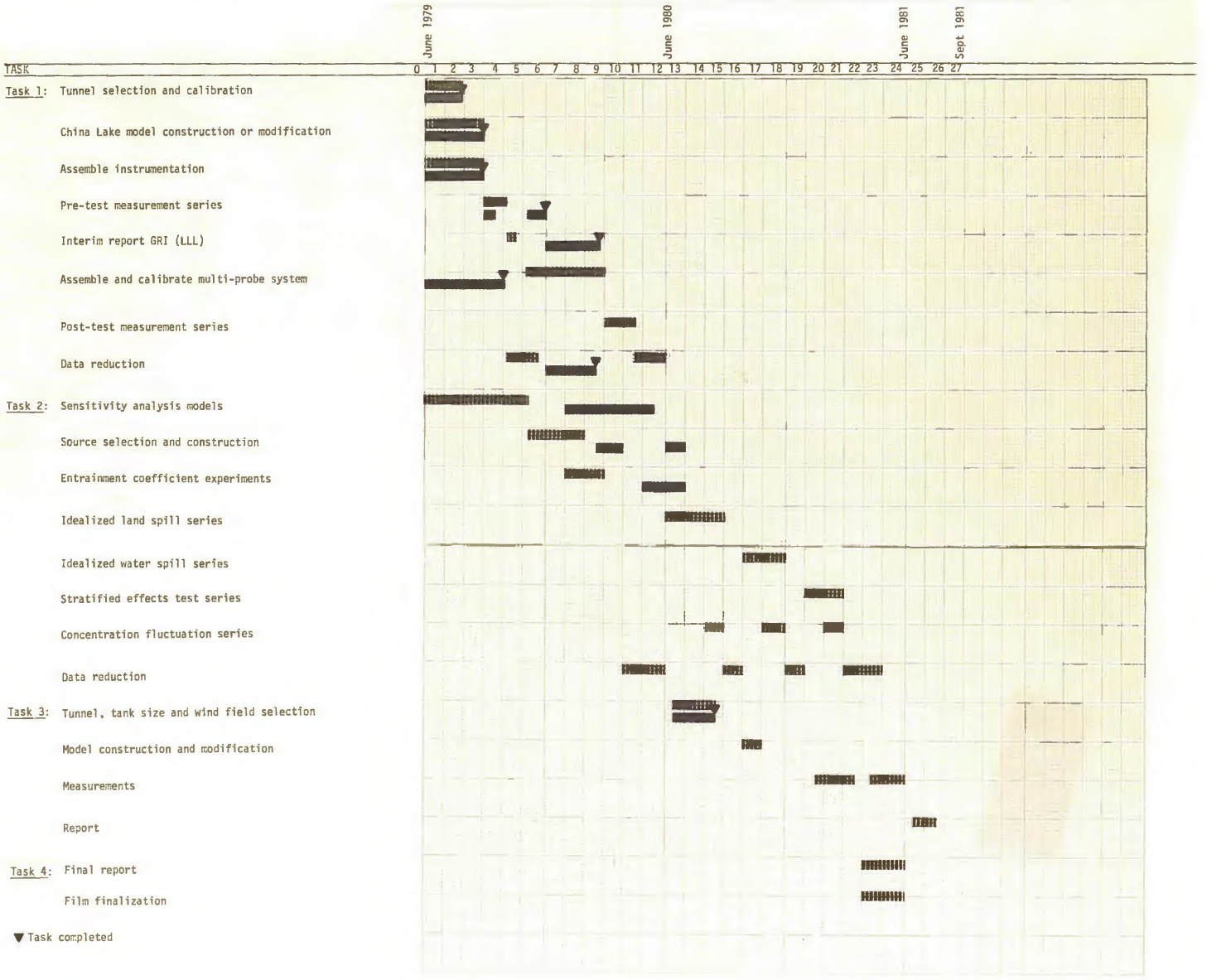

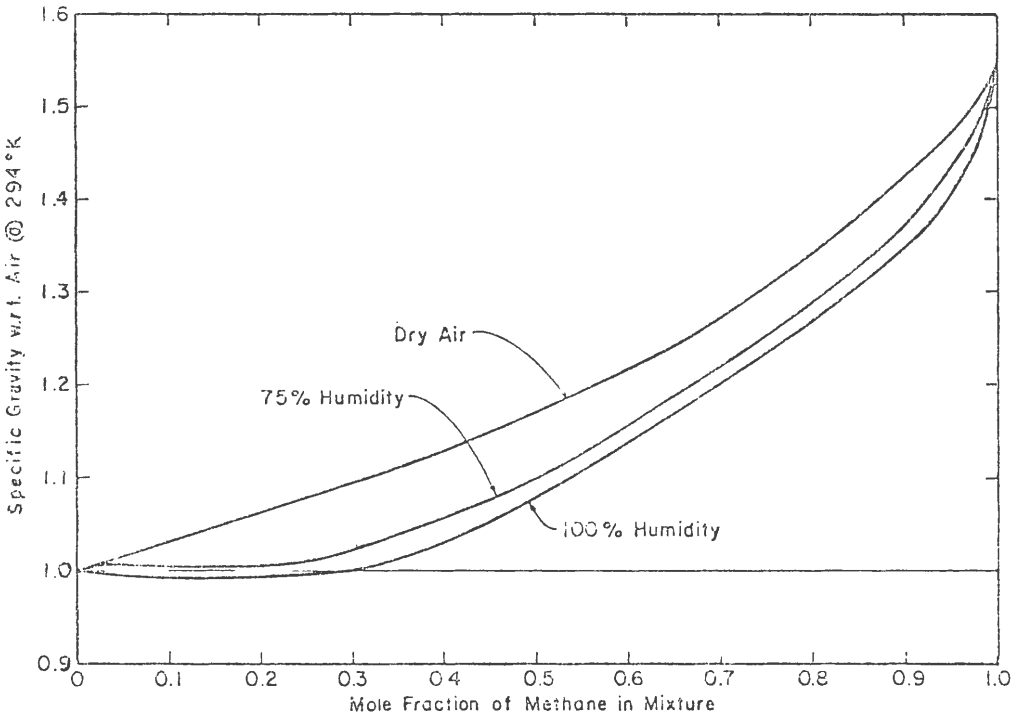

Figure 1. Specific Gravity of LNG Vapor - Humid Atmosphere Mixtures

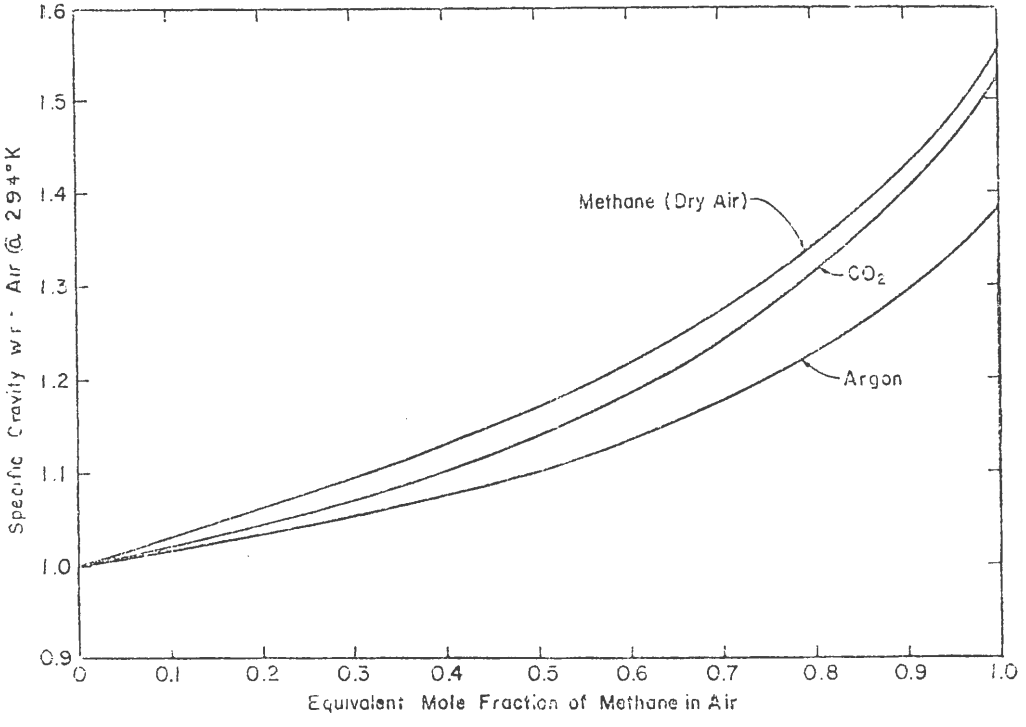

Figure 2. Specific Gravity of Gas-Air Mixtures

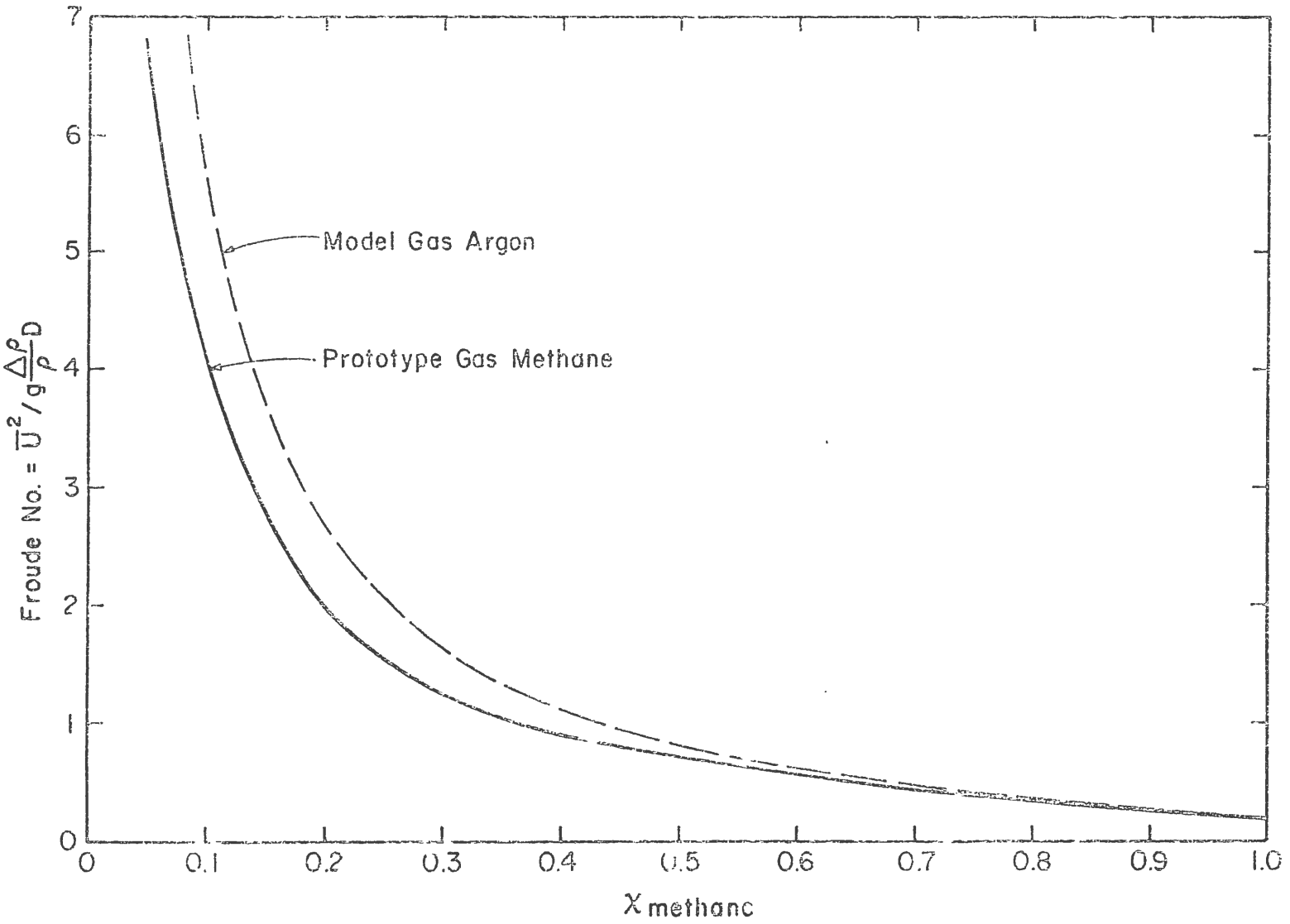

Figure 3. Variation of Froude Number for Gas-Air Mixtures

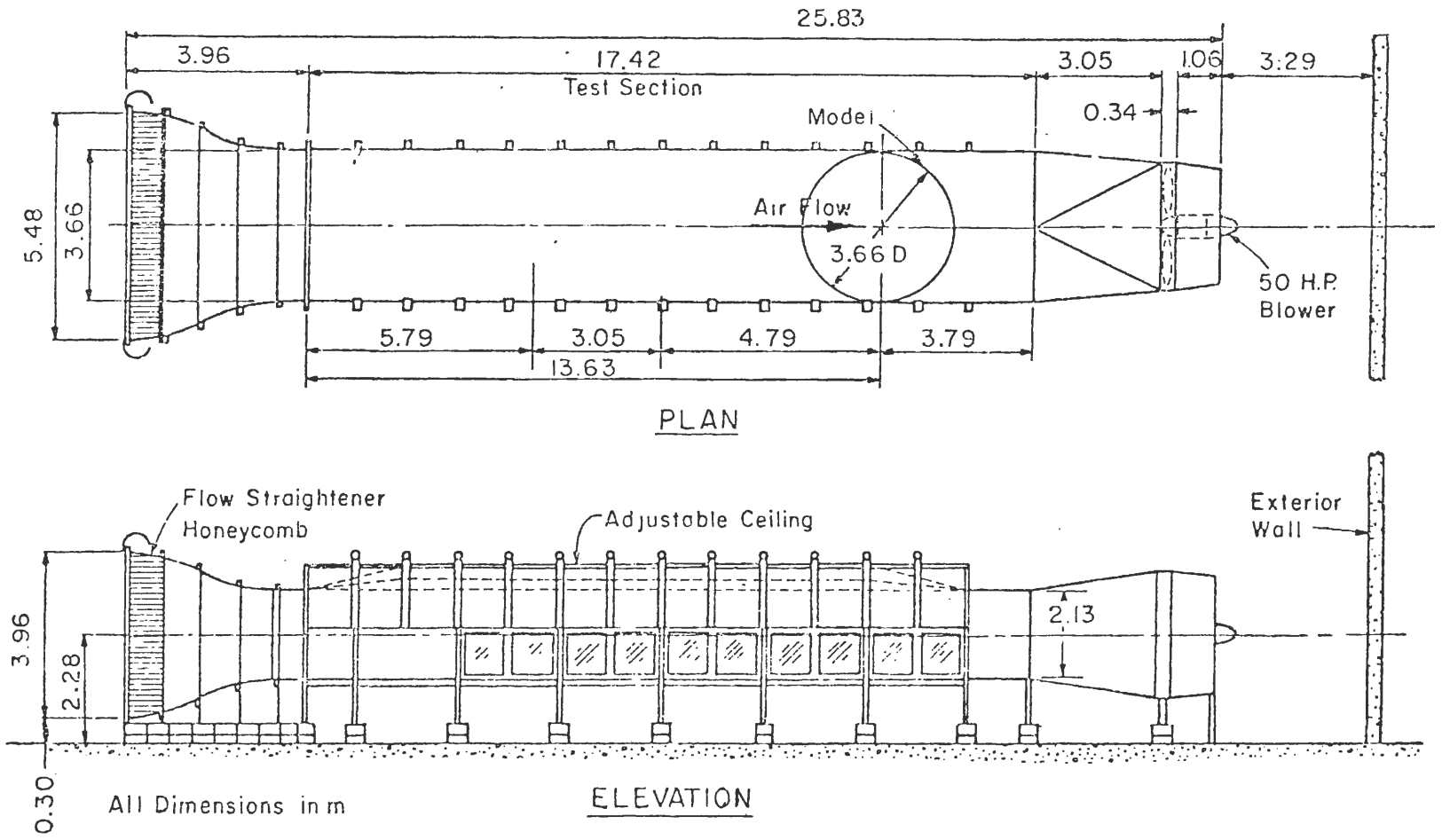

Figure 4. Environmental Wind Tunnel

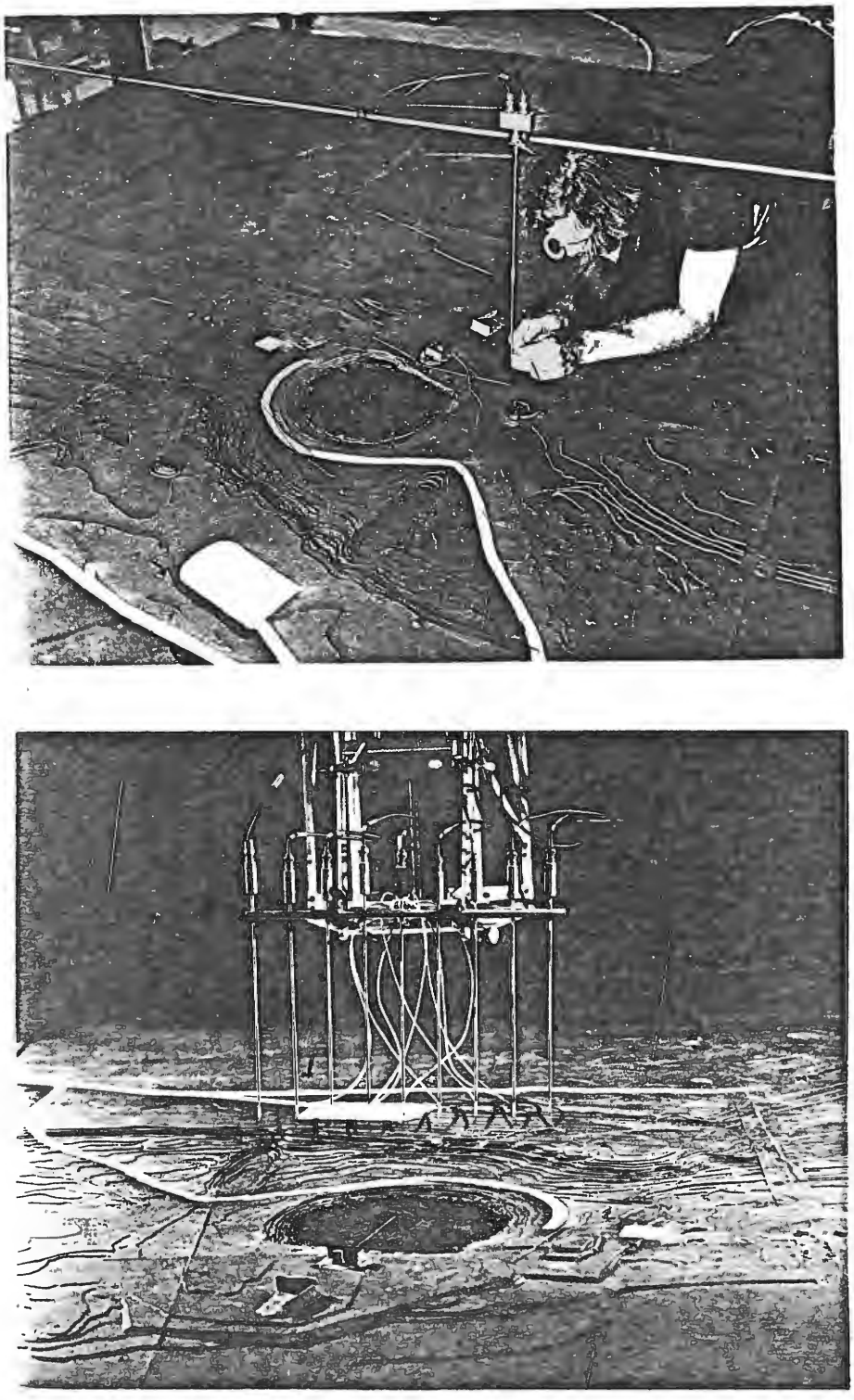

Figure 5. China Lake Naval Weapons Center Spill Site Model; Scale 1:240

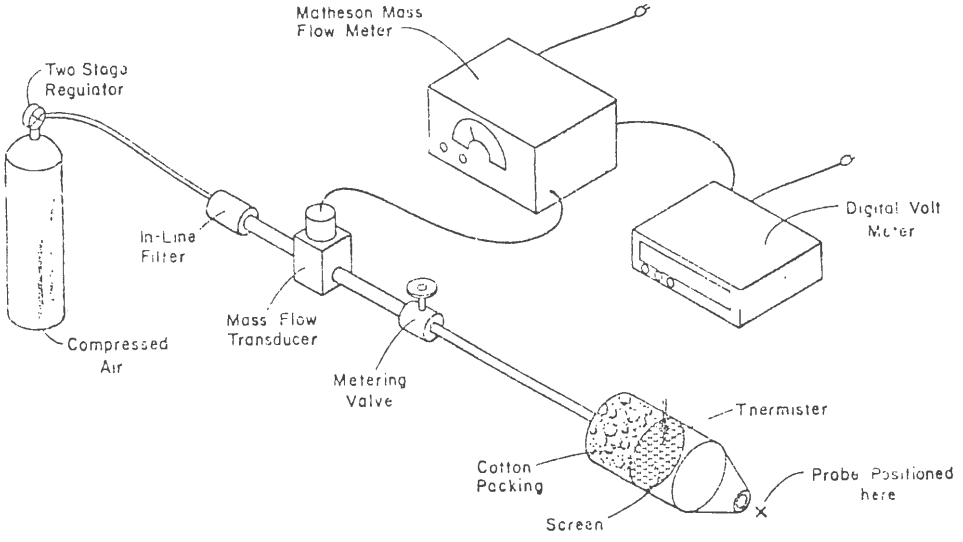

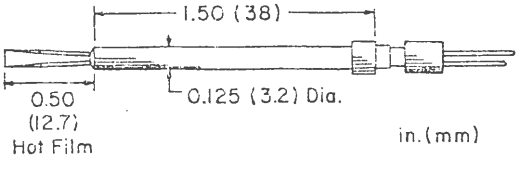

TSI Single Film Sensor

Figure 6. Velocity Probes and Velocity Standard

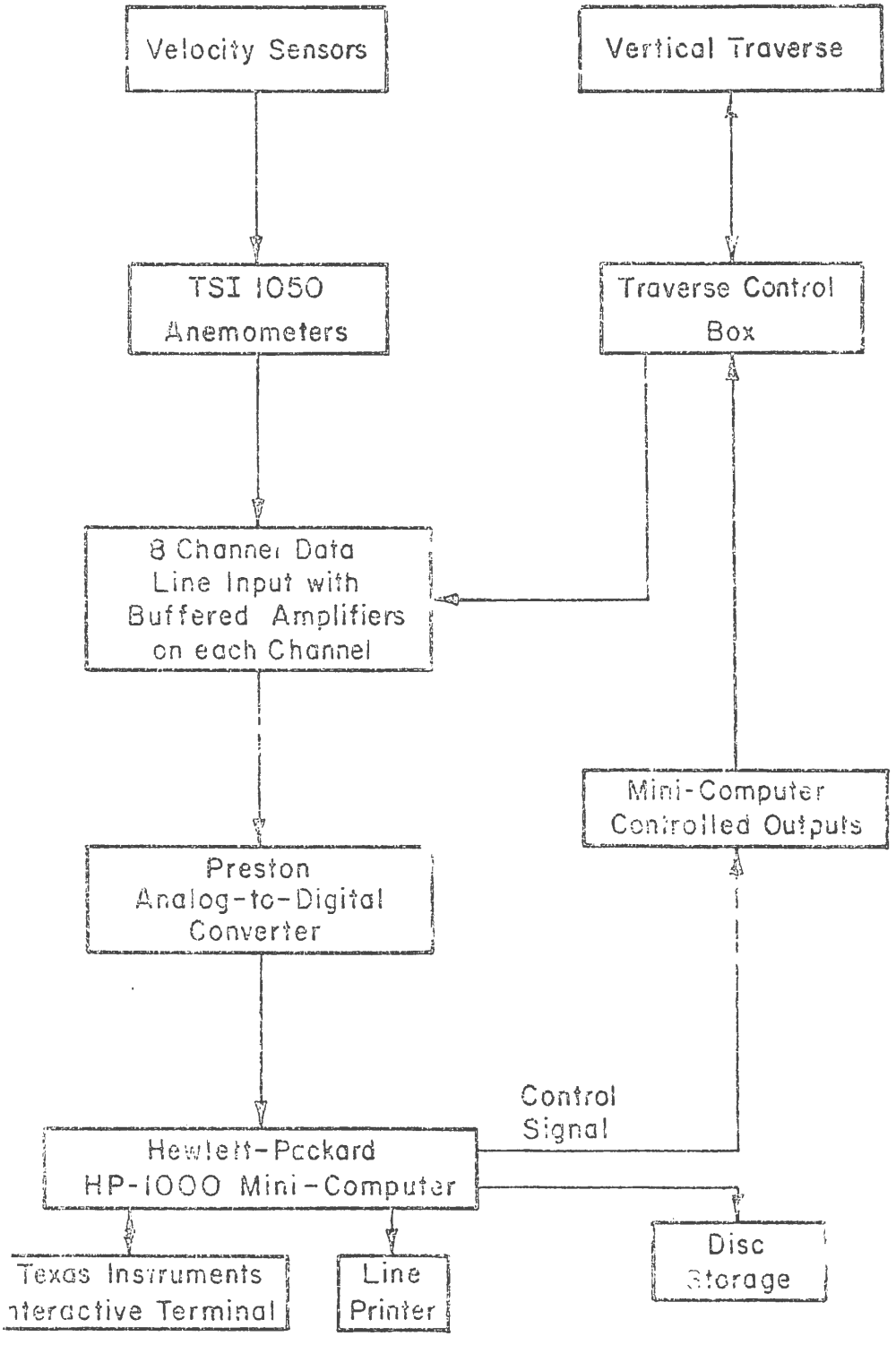

Figure 7. Velocity Data Reduction Flow Chart

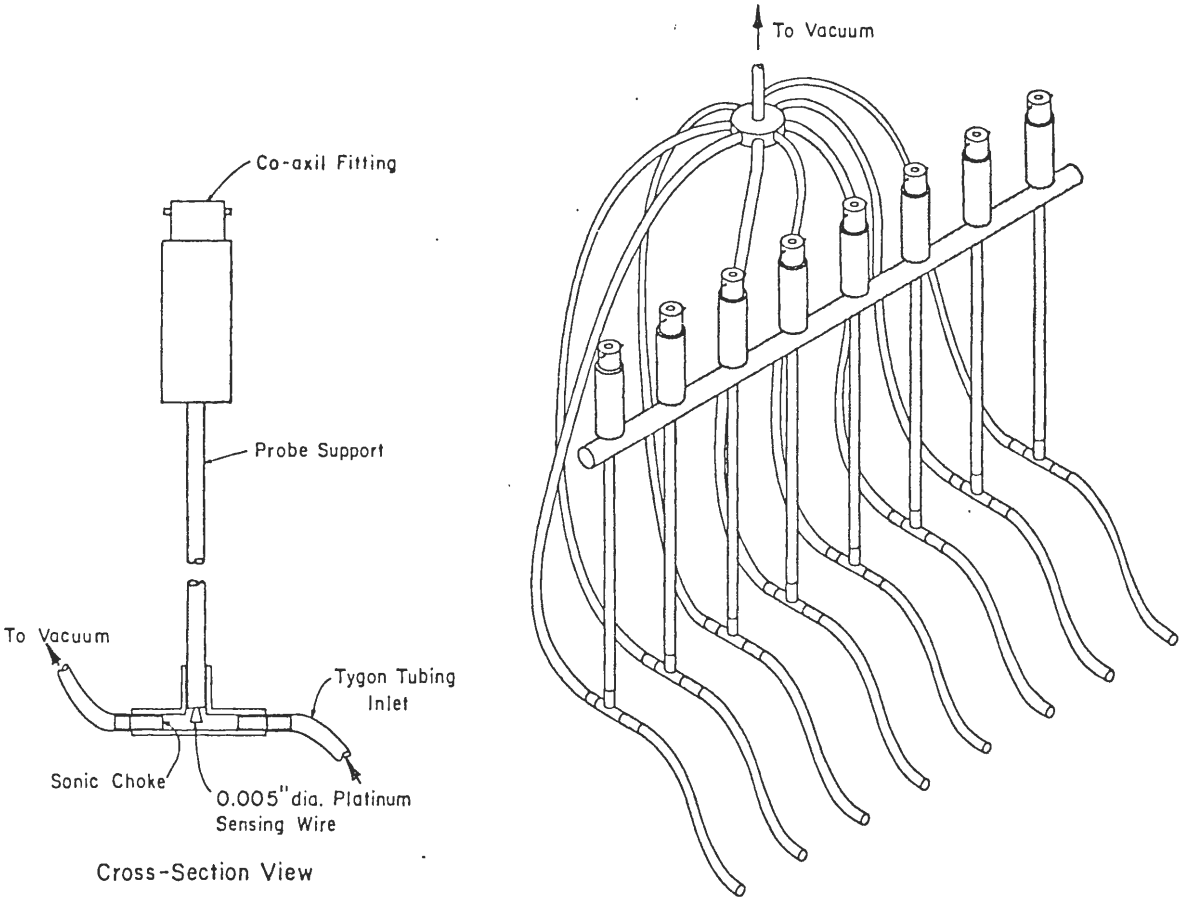

Figure 8. Hot-Wire Katharometer Probes

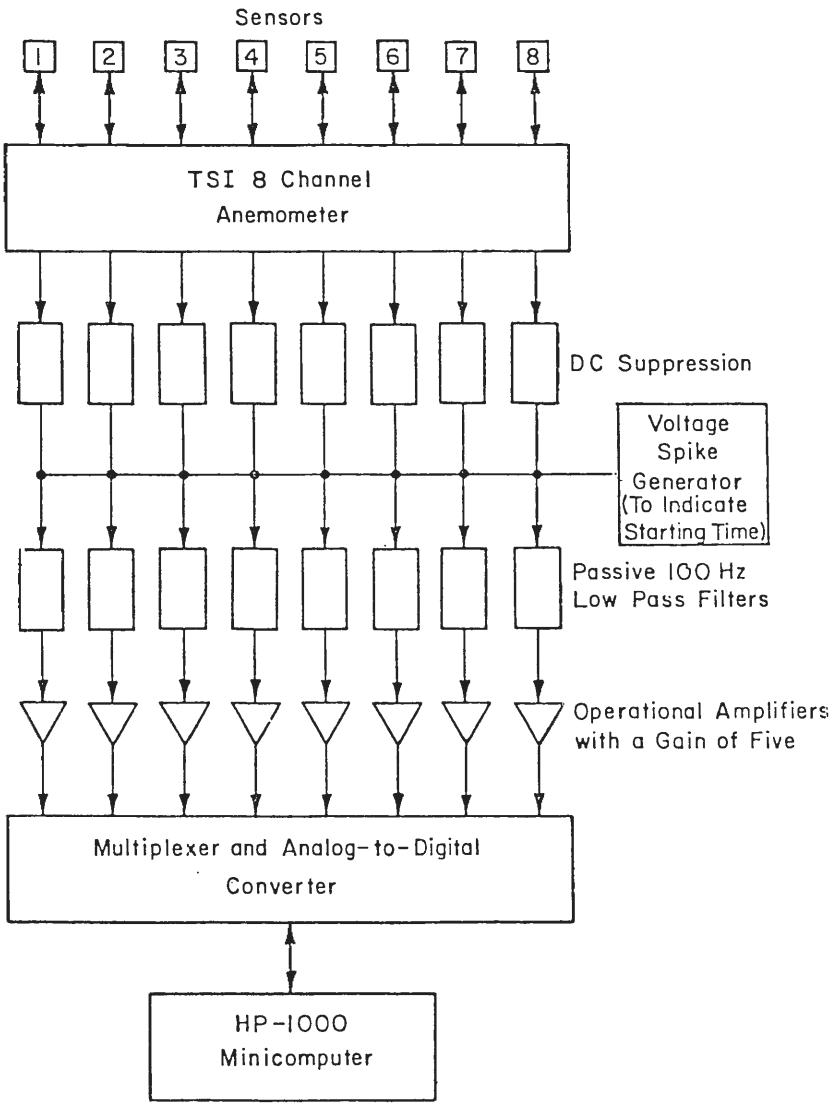

Figure 9. Block Diagram Katharometer Array

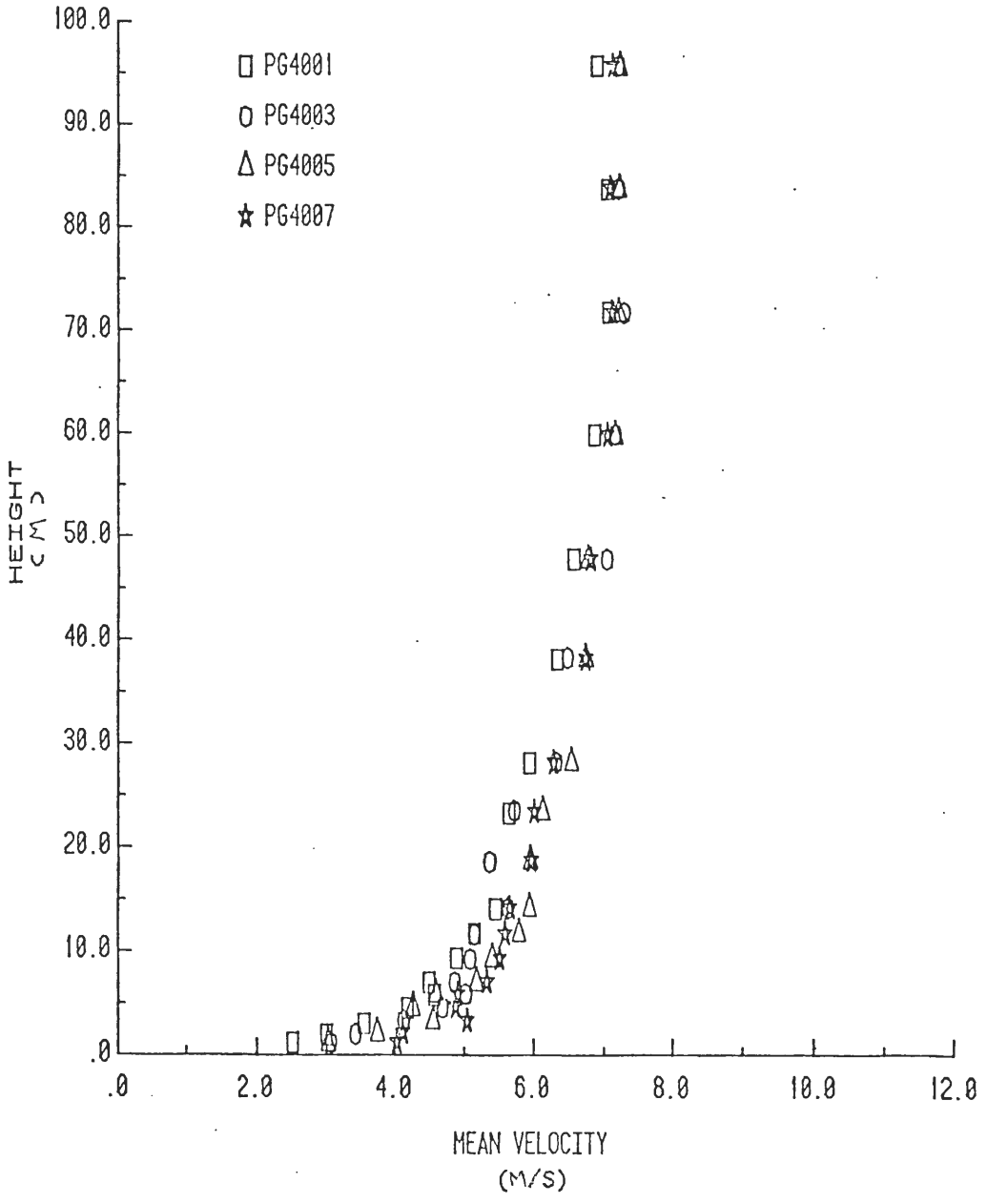

Figure 10. Mean Longitudinal Velocity Profiles

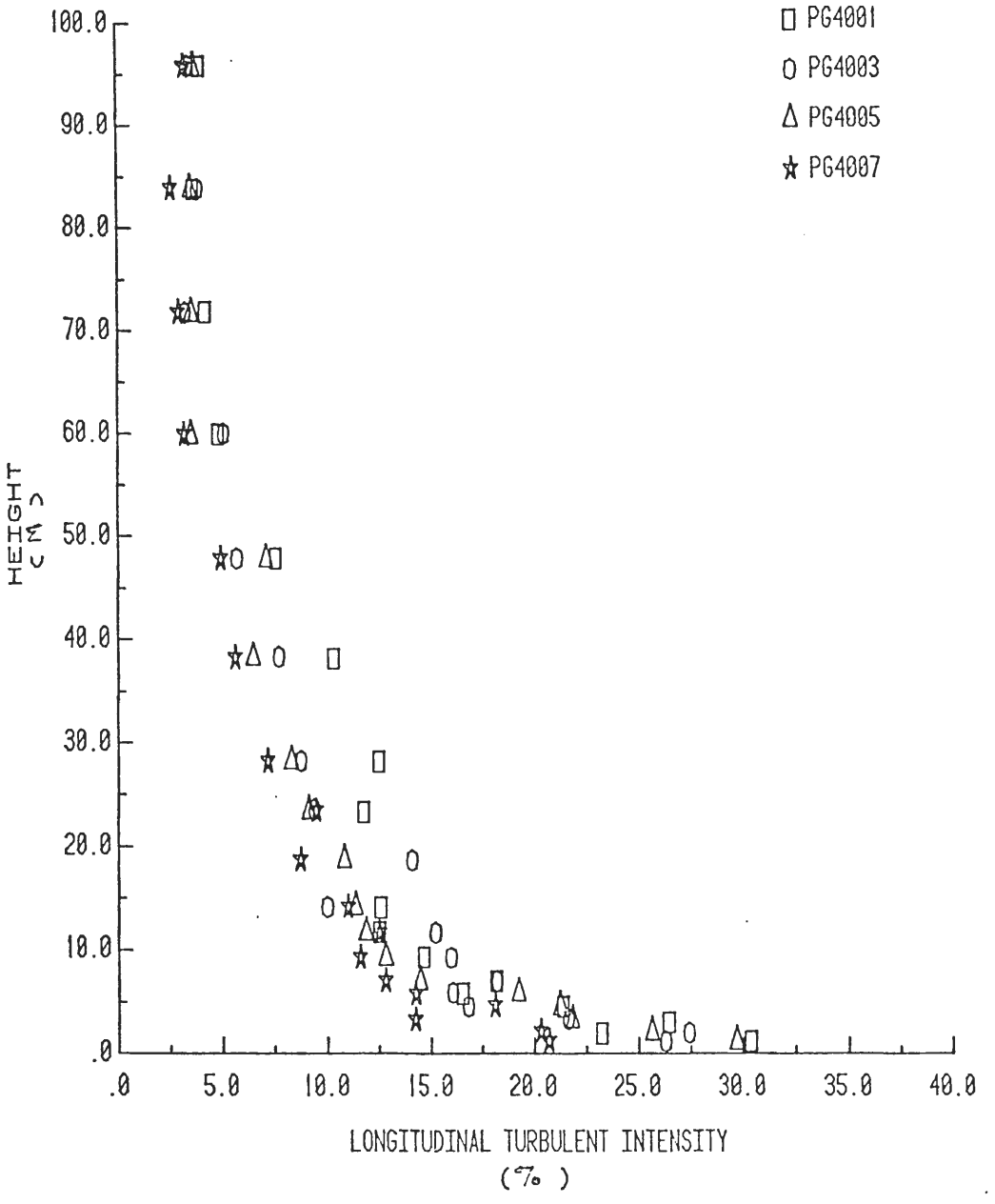

Figure 11. Local Longitudinal Turbulent Intensity Profiles

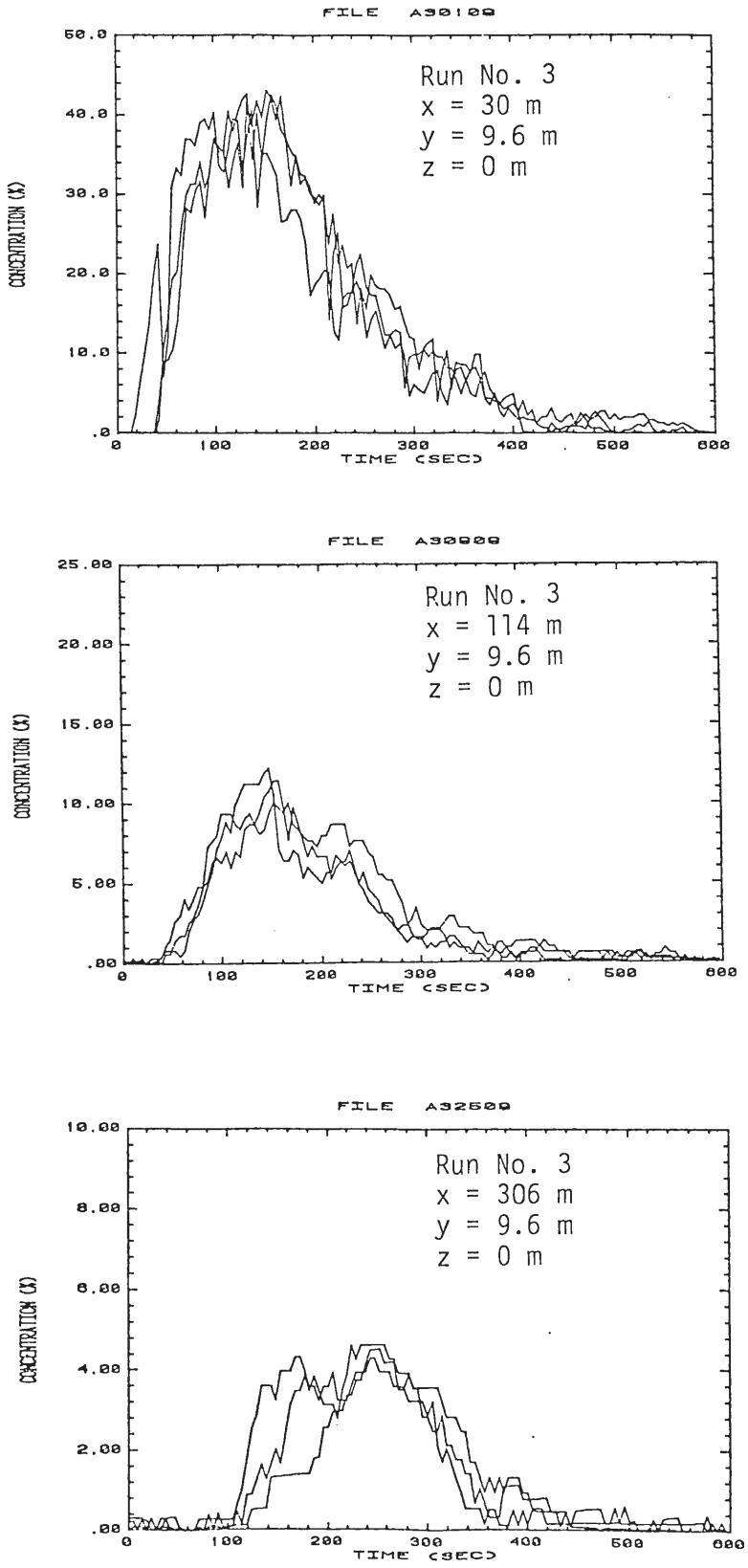

Figure 12. Concentration Time Histories

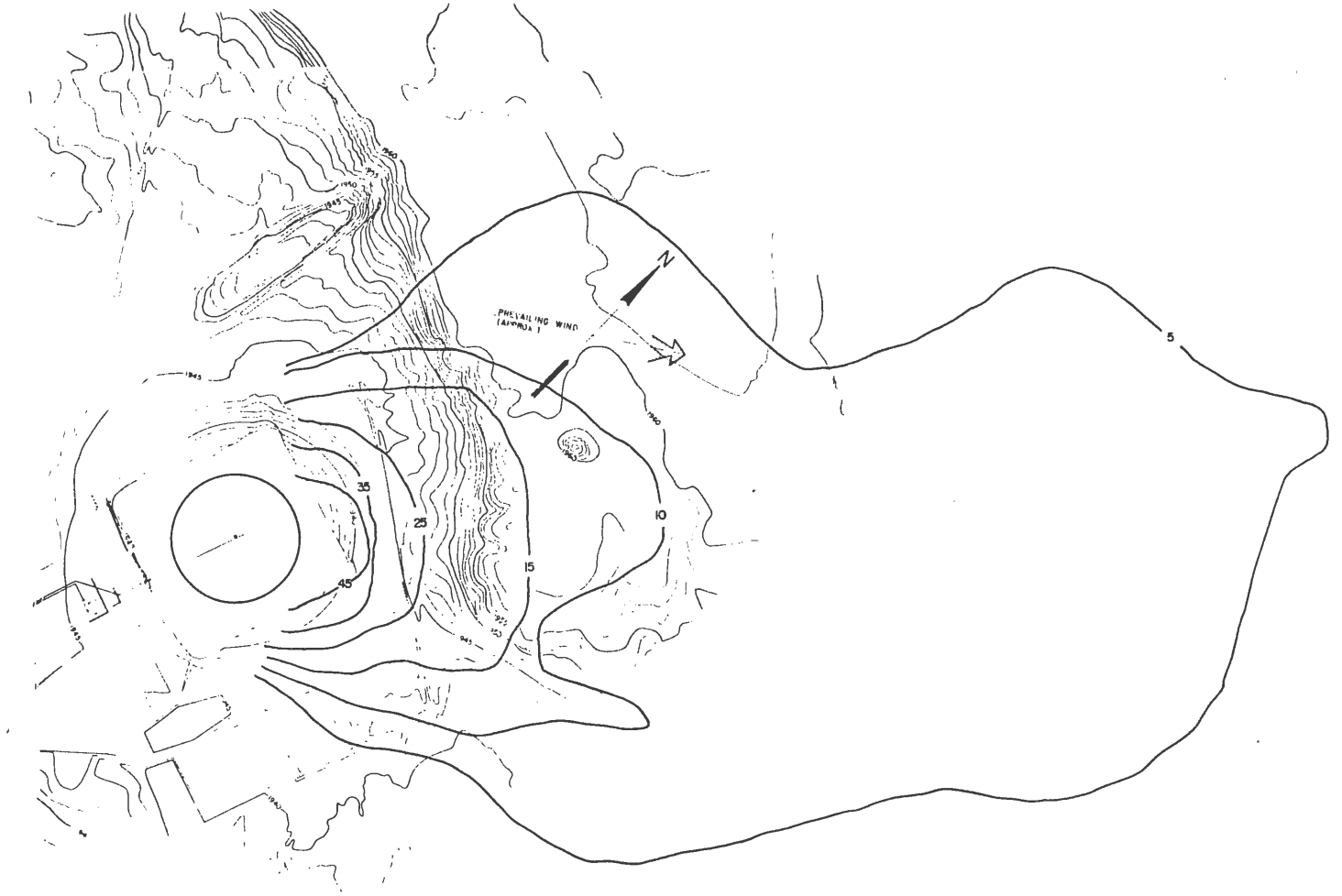

Figure 13-1. Ground Level Peak Concentration Contours (Run No. 1)

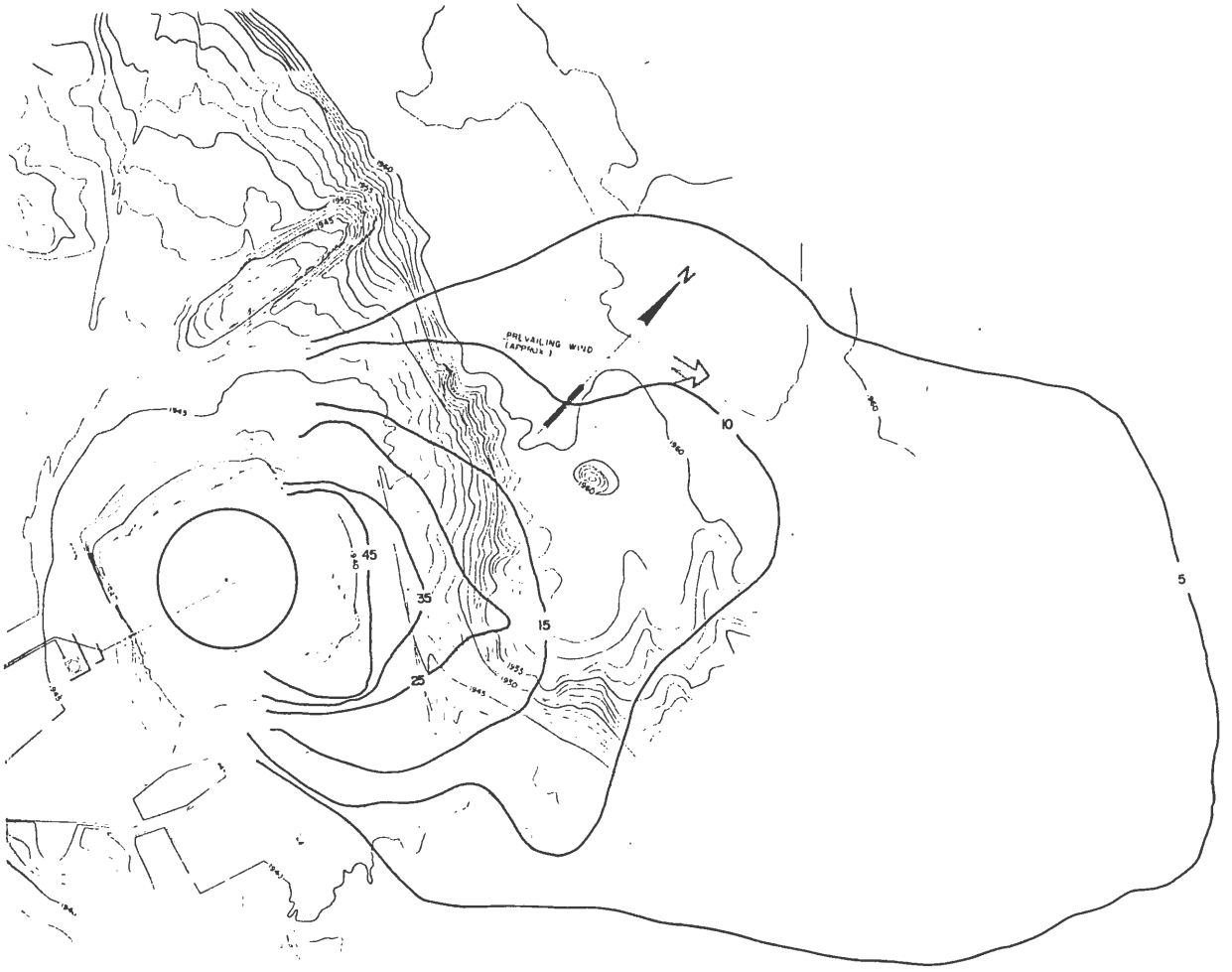

Figure 13-2. Ground Level Peak Concentration Contours (Run No. 2)

Figure 13-3. Ground Level Peak Concentration Contours (Run No. 3)

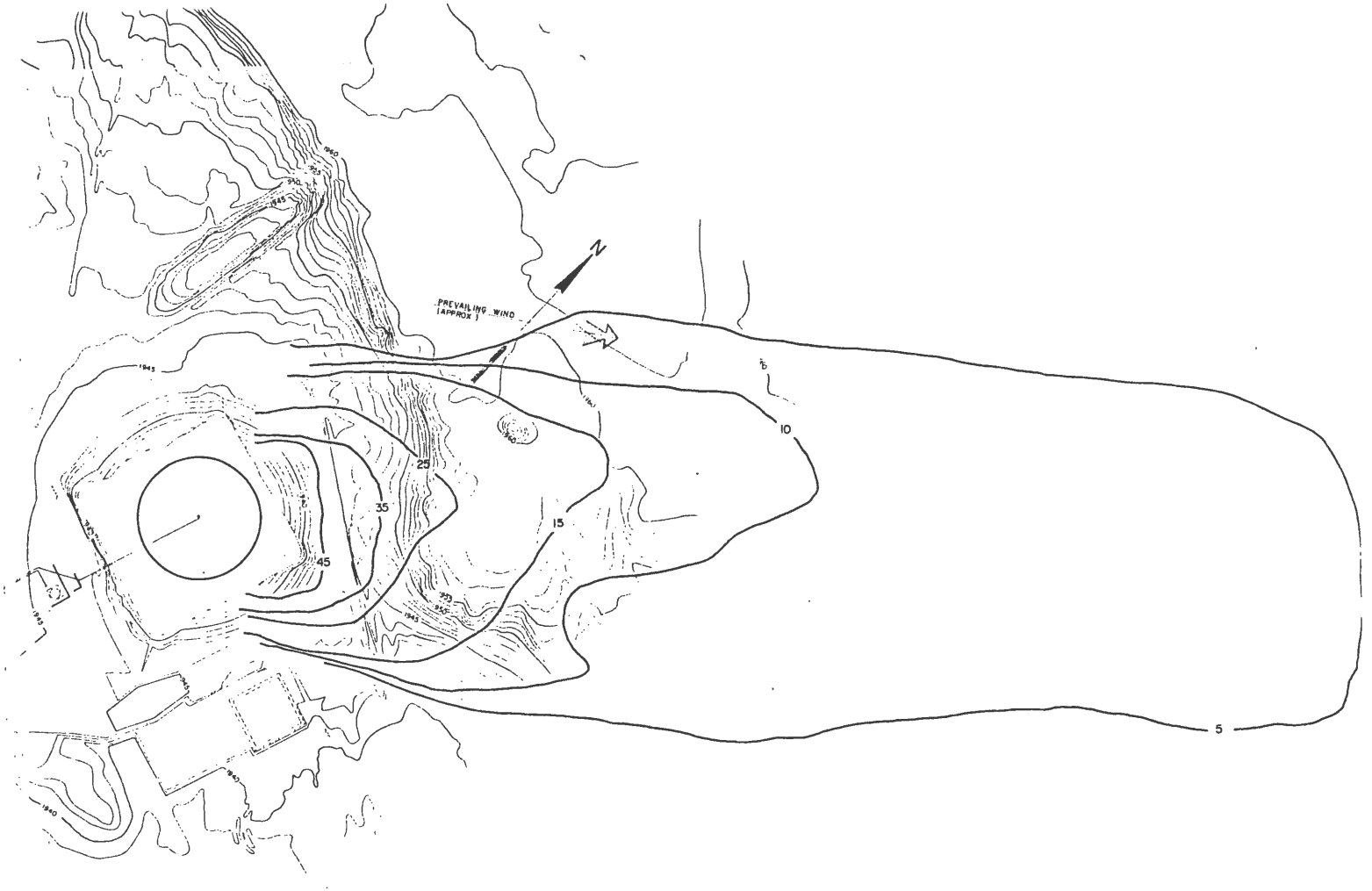

Figure 13-4. Ground Level Peak Concentration Contours (Run No. 4)

Figure 13-5. Ground Level Peak Concentration Contours (Run No. 5)

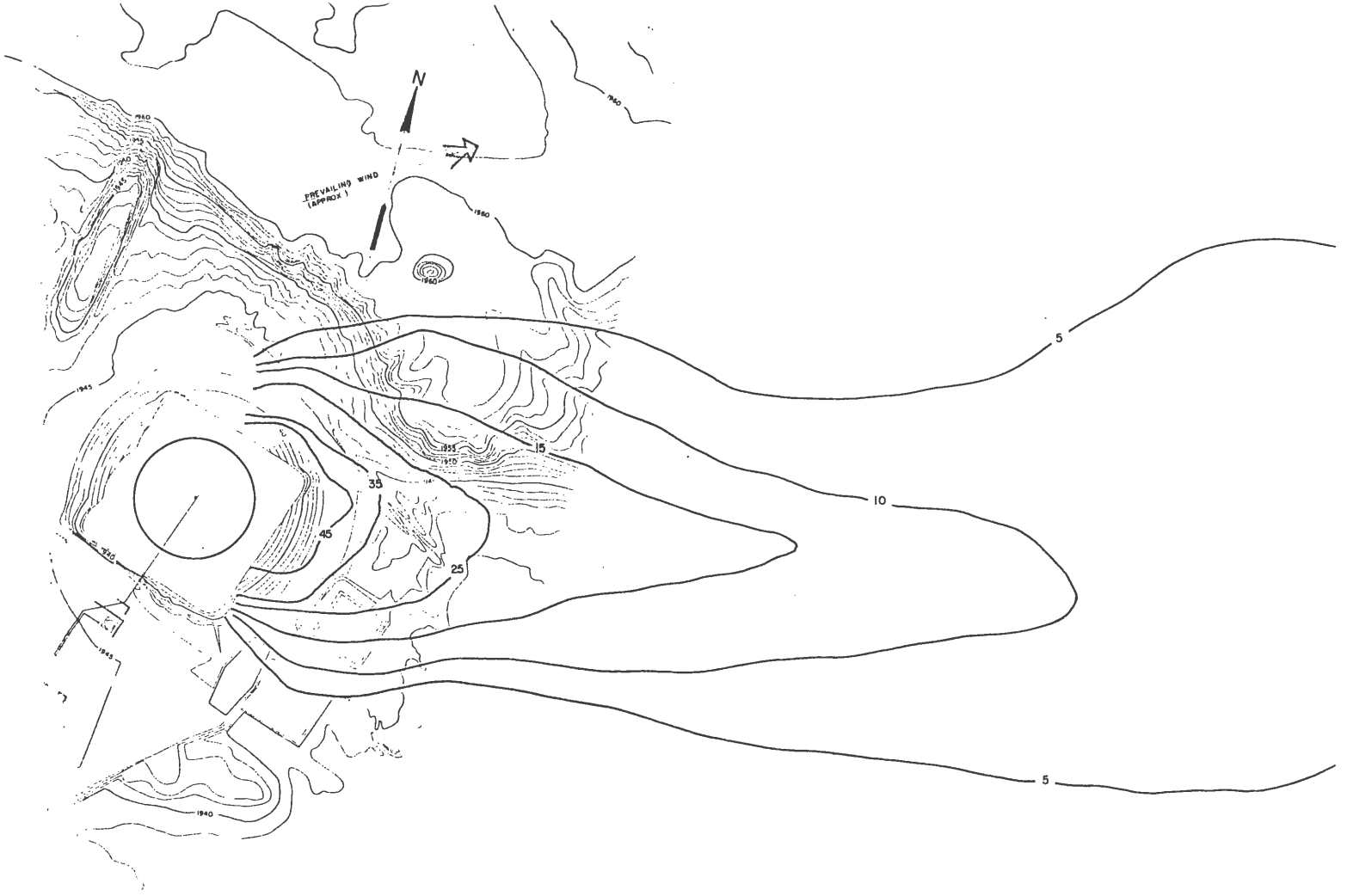

Figure 13-6. Ground Level Peak Concentration Contours (Run No. 6)

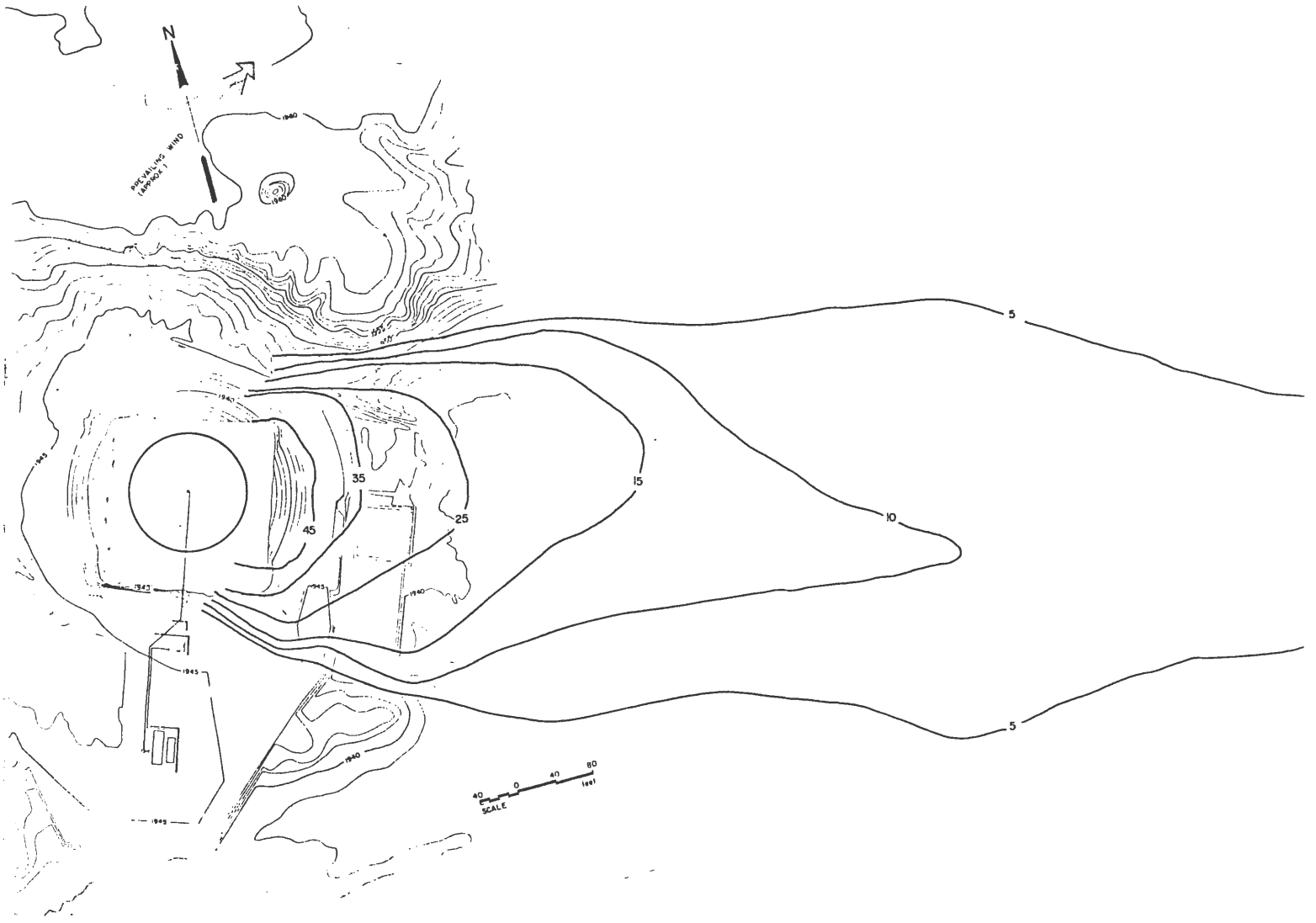

Figure 13-7. Ground Level Peak Concentration Contours (Run No. 7)

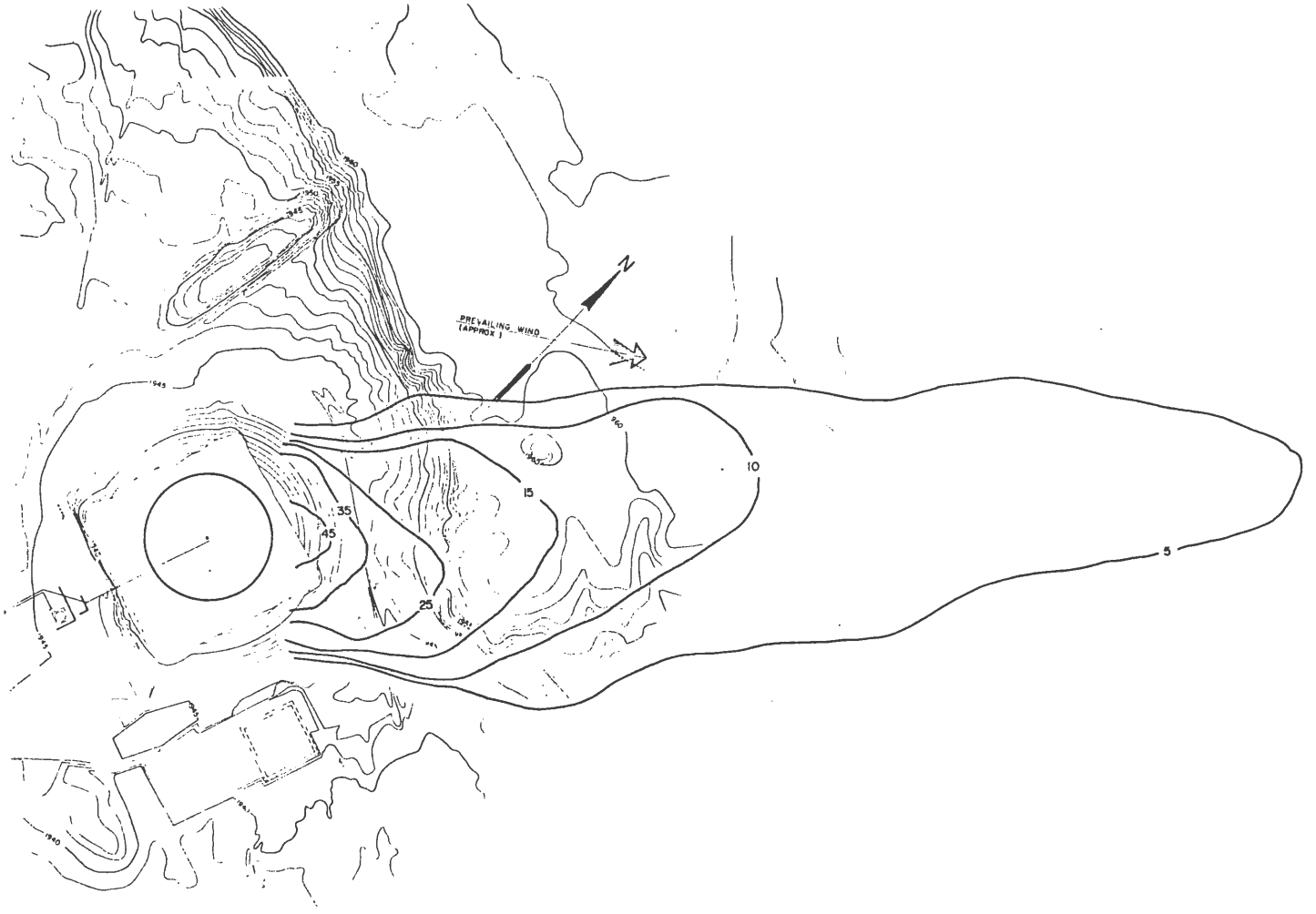

Figure 13-8. Ground Level Peak Concentration Contours (Run No. 8)

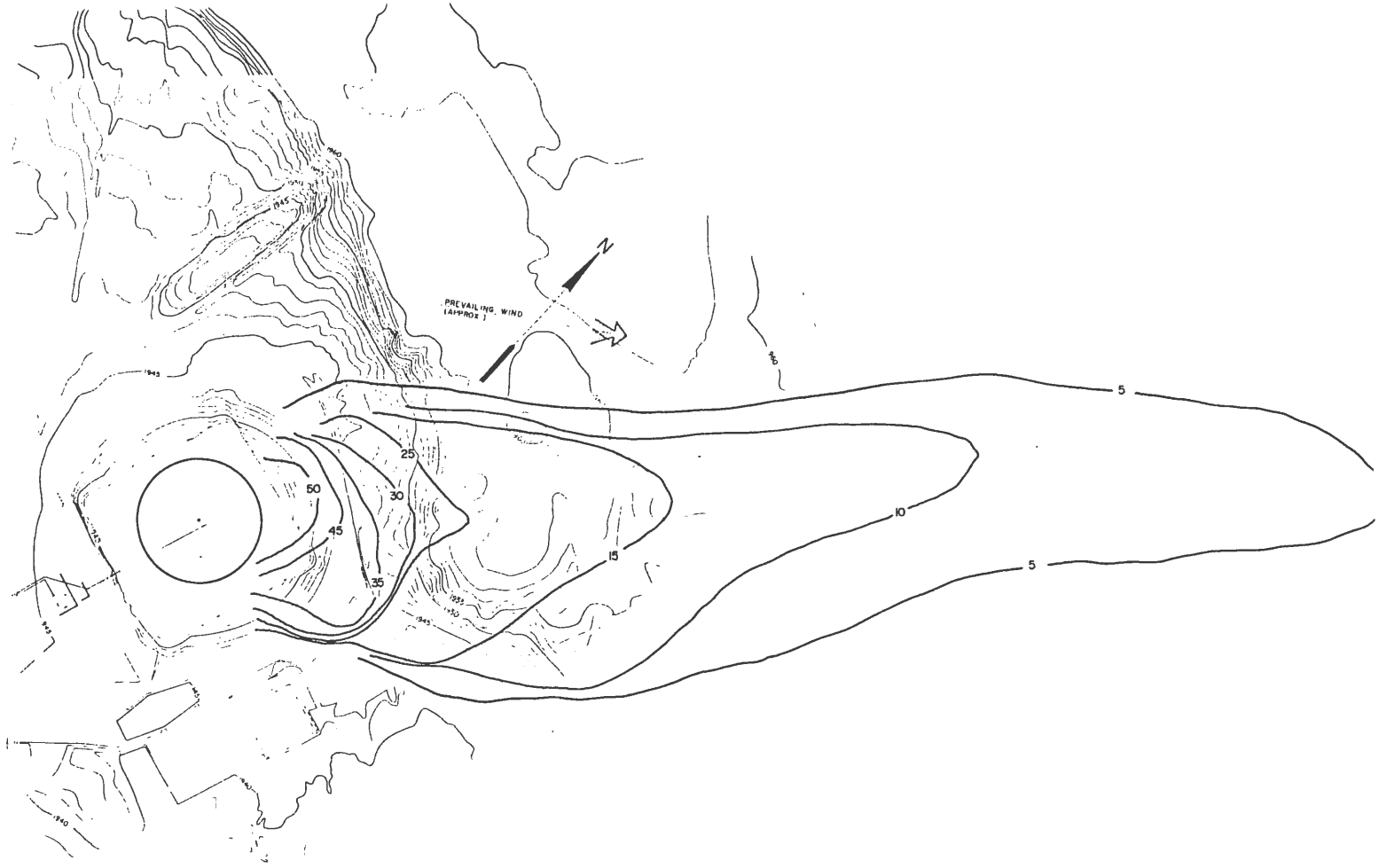

Figure 13-9. Ground Level Peak Concentration Contours (Run No. 9)

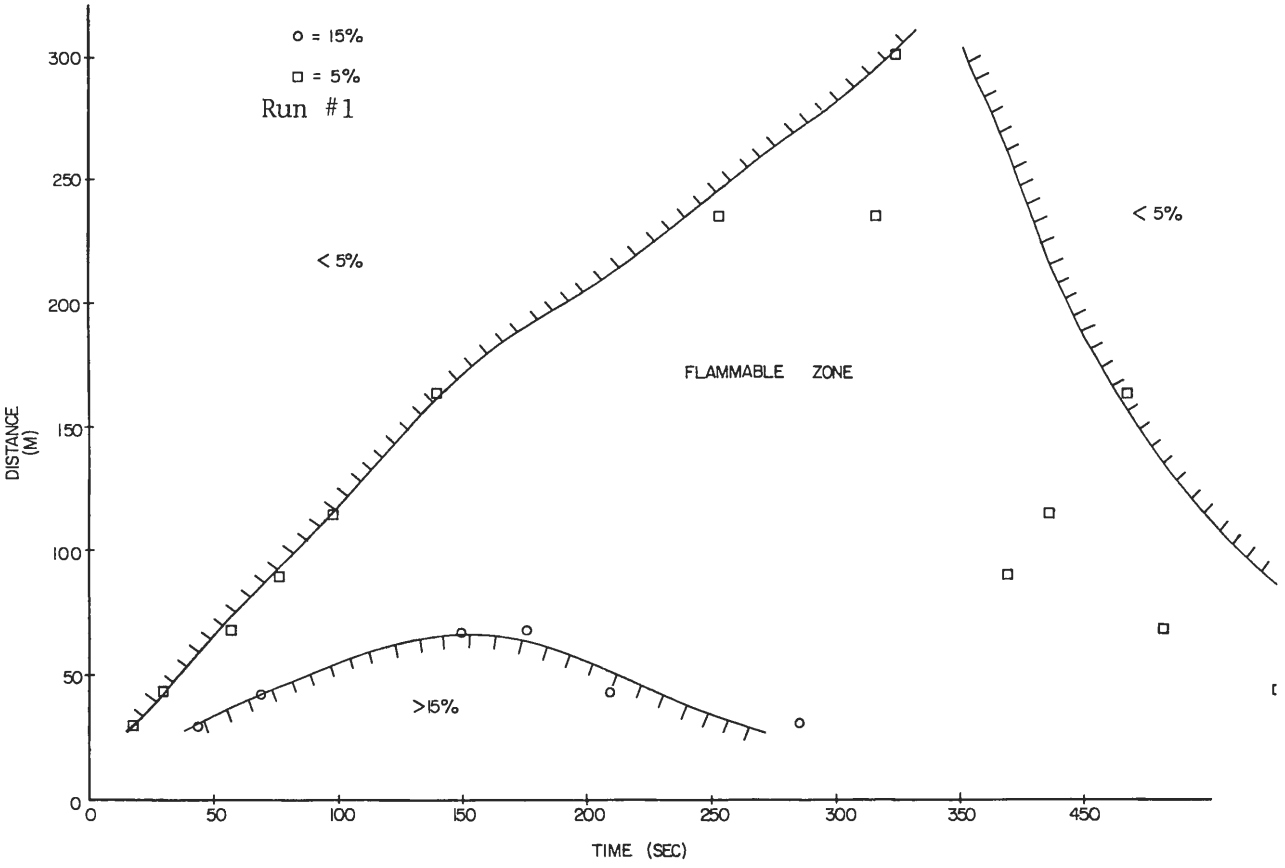

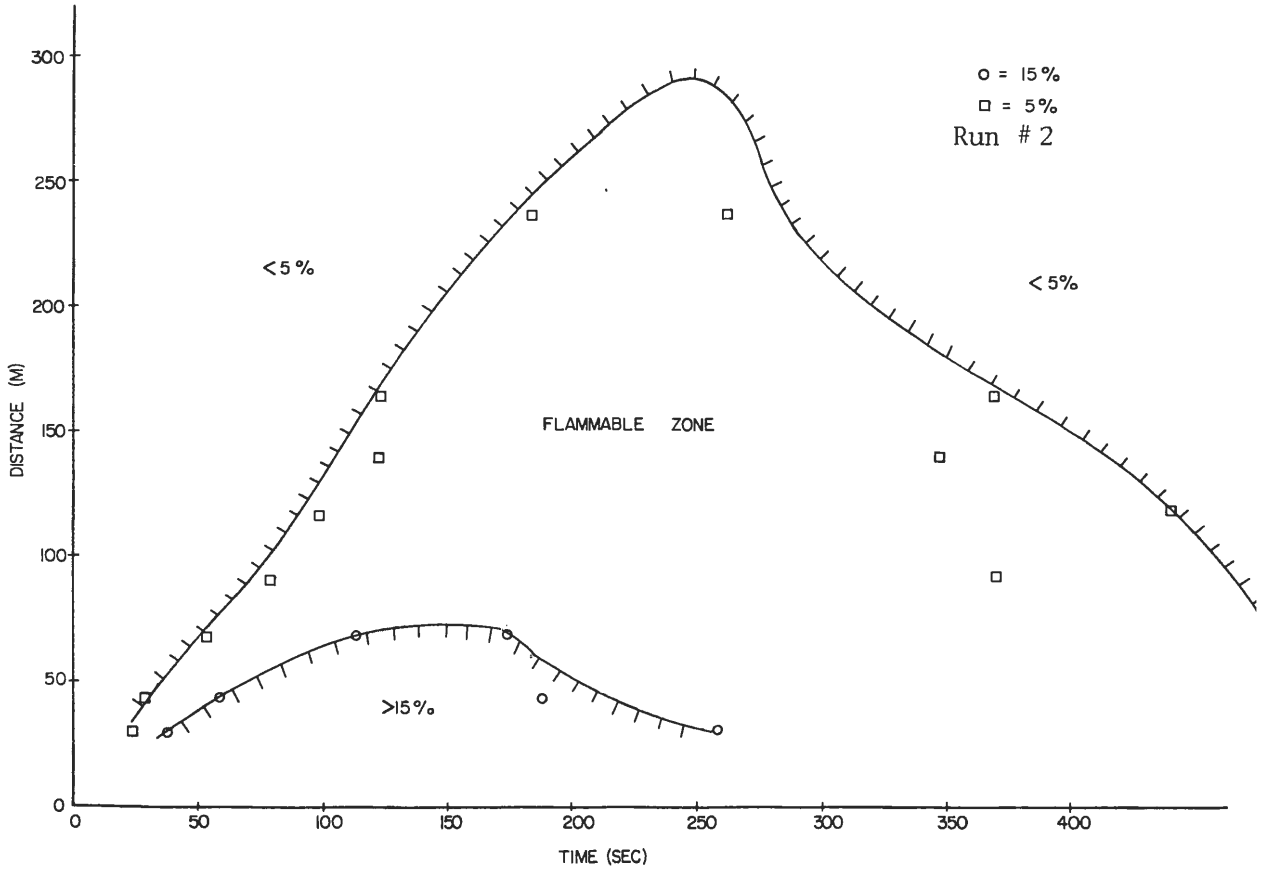

Figure 14-1. Maximum Limits of Flammable Zone as a Function of Distance and Time

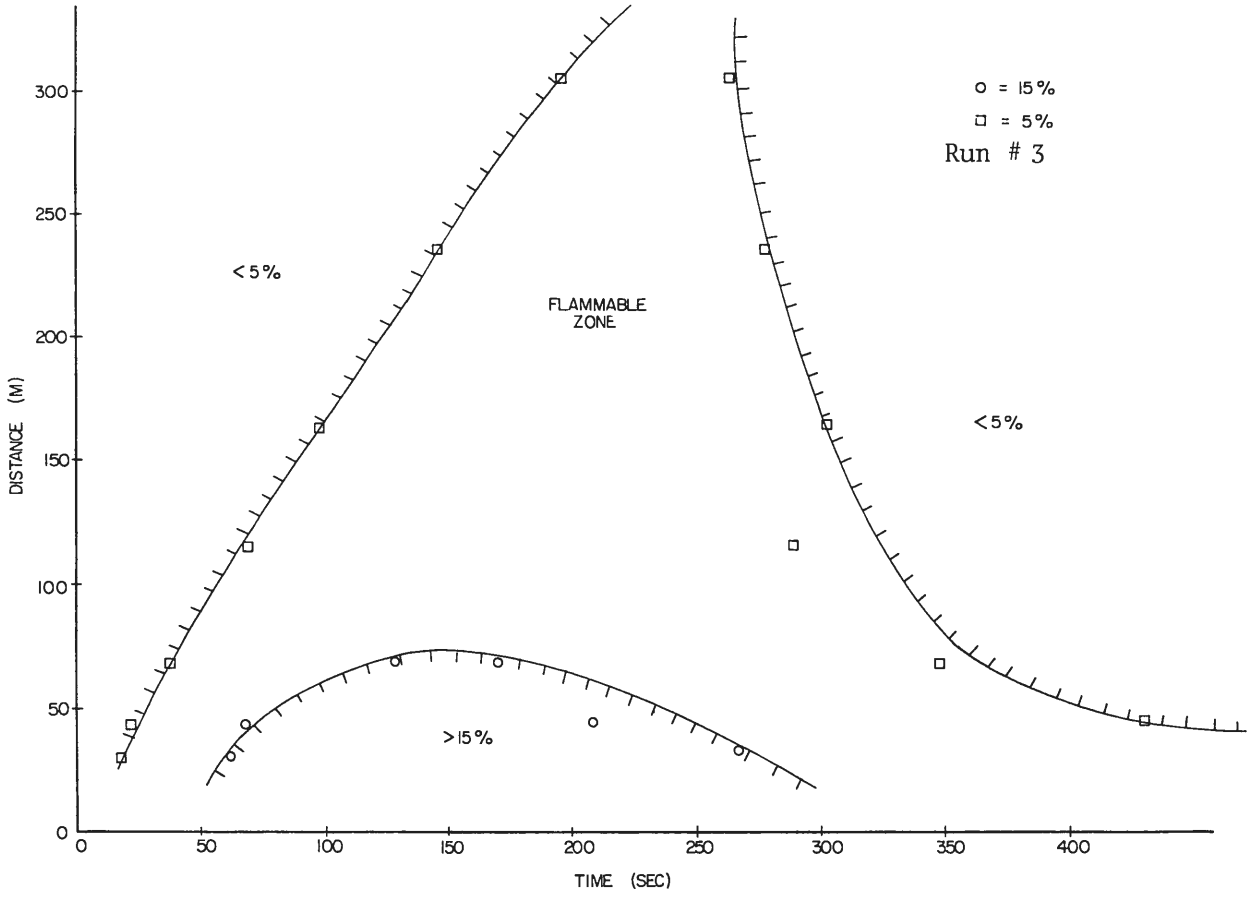

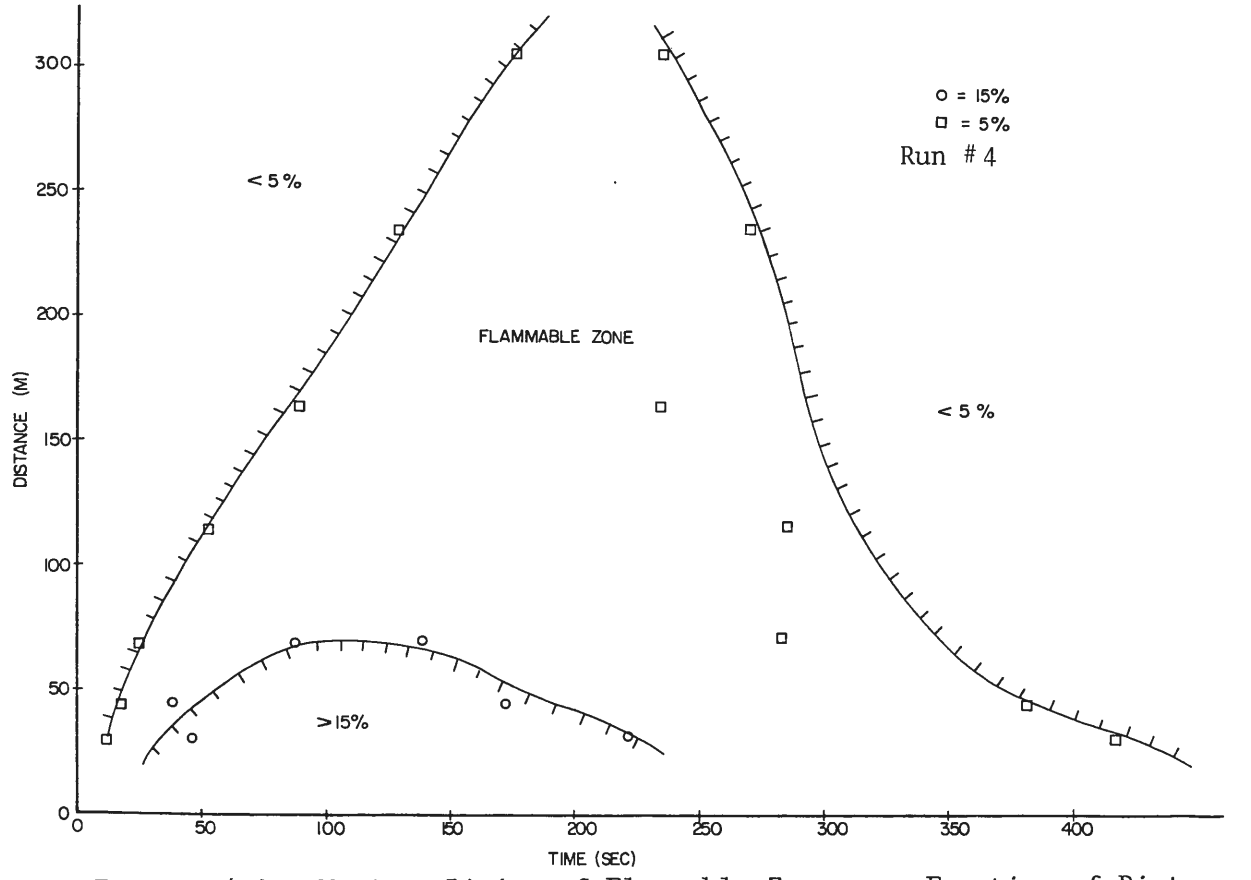

Figure 14-2. Maximum Limits of Flammable Zone as a Function of Distance and Time

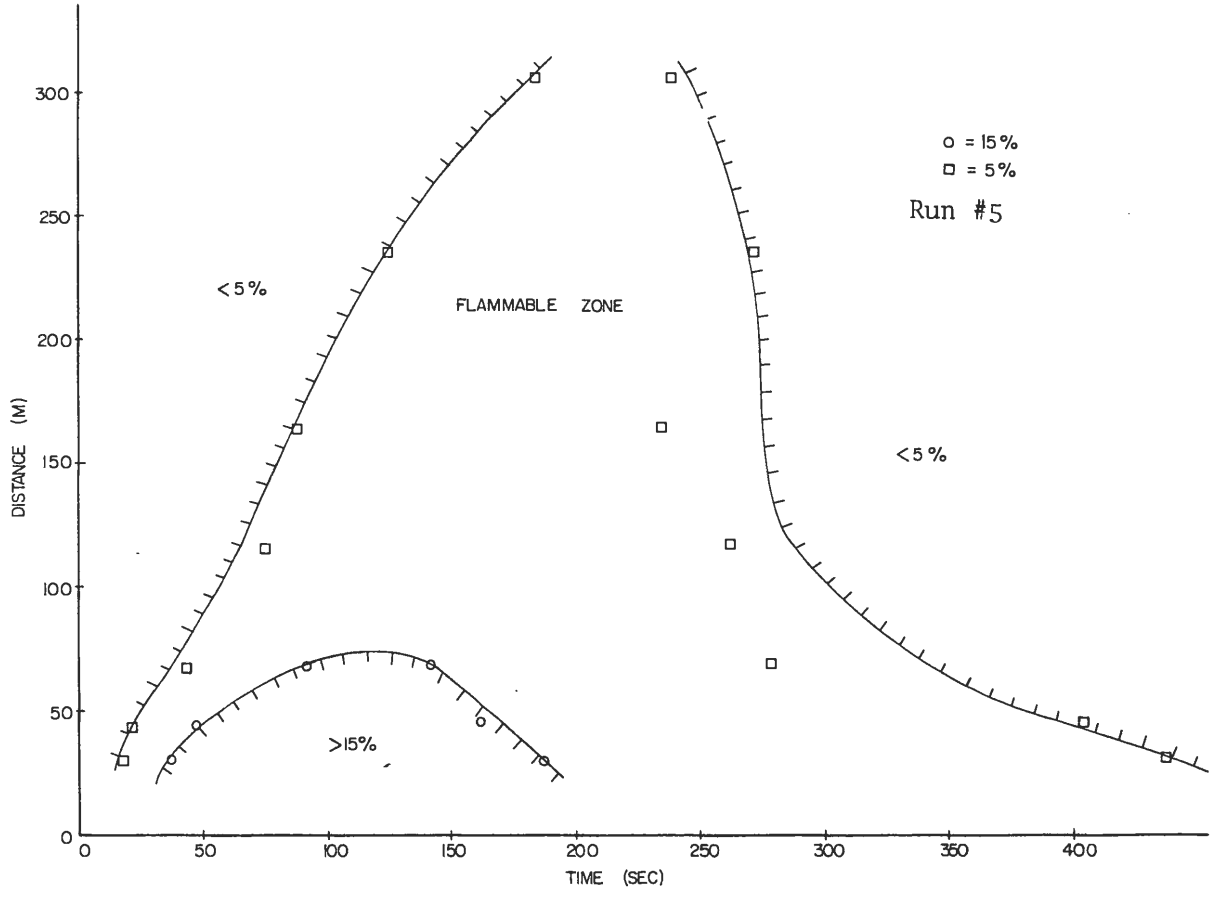

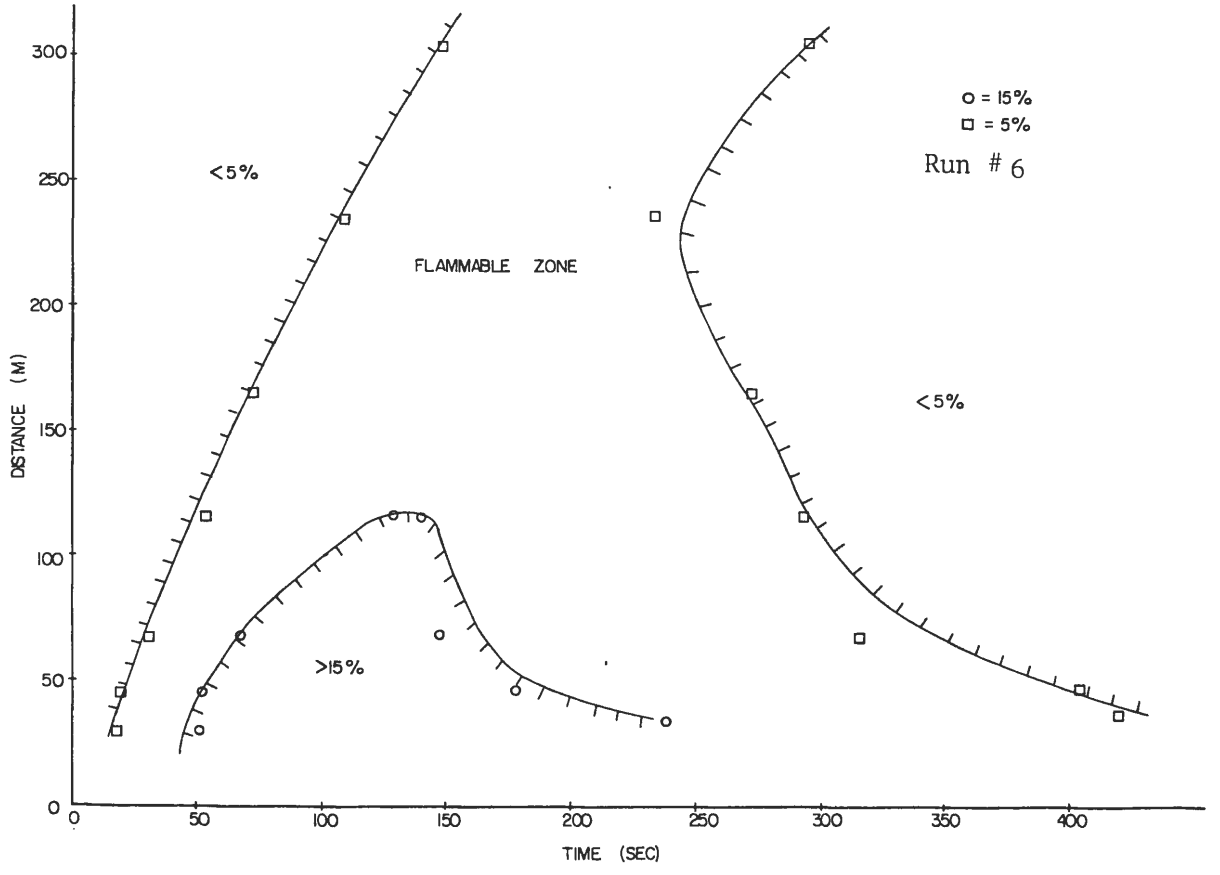

Figure 14-3. Maximum Limits of Flammable Zone as a Function of Distance and Time

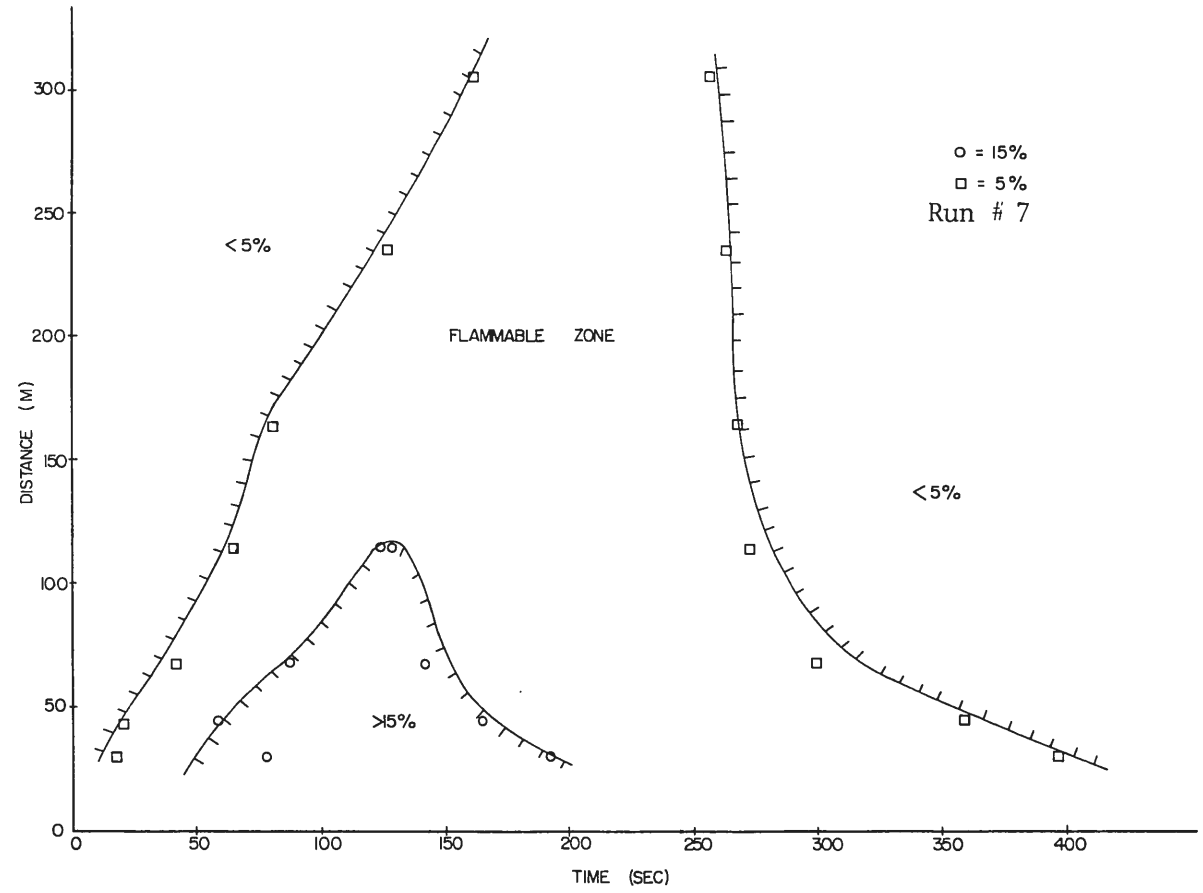

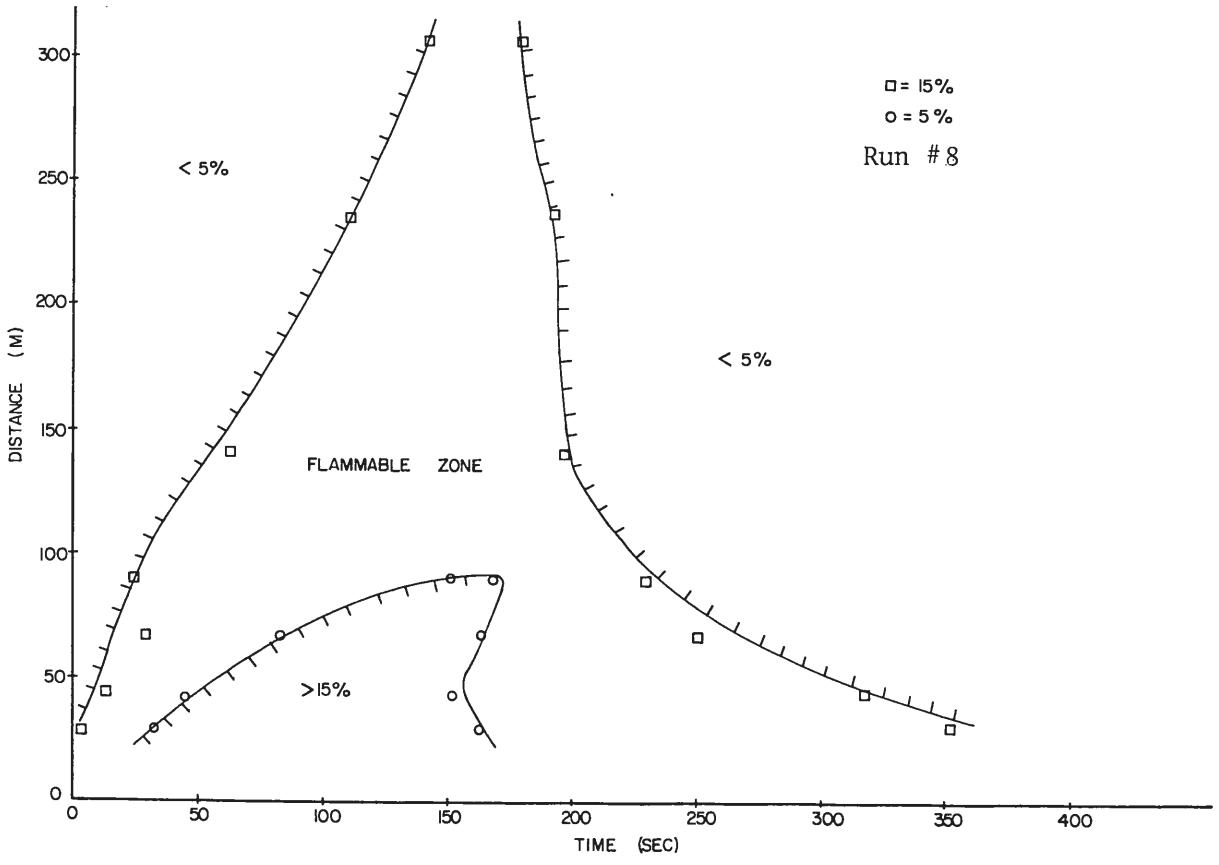

Figure 14-4. Maximum Limits of Flammable Zone as a Function of Distance and Time

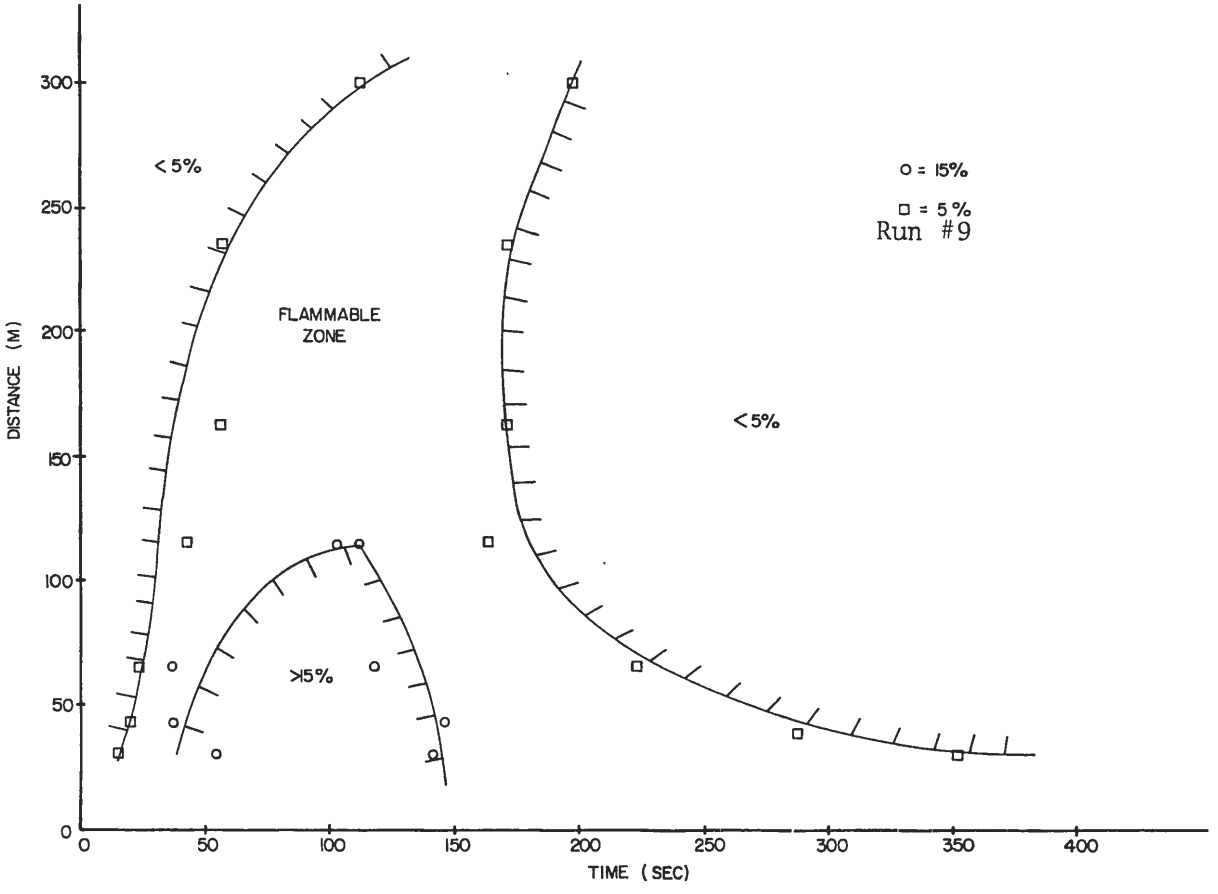

Figure 14-5. Maximum Limits of Flammable Zone as a Function of Distance and Time

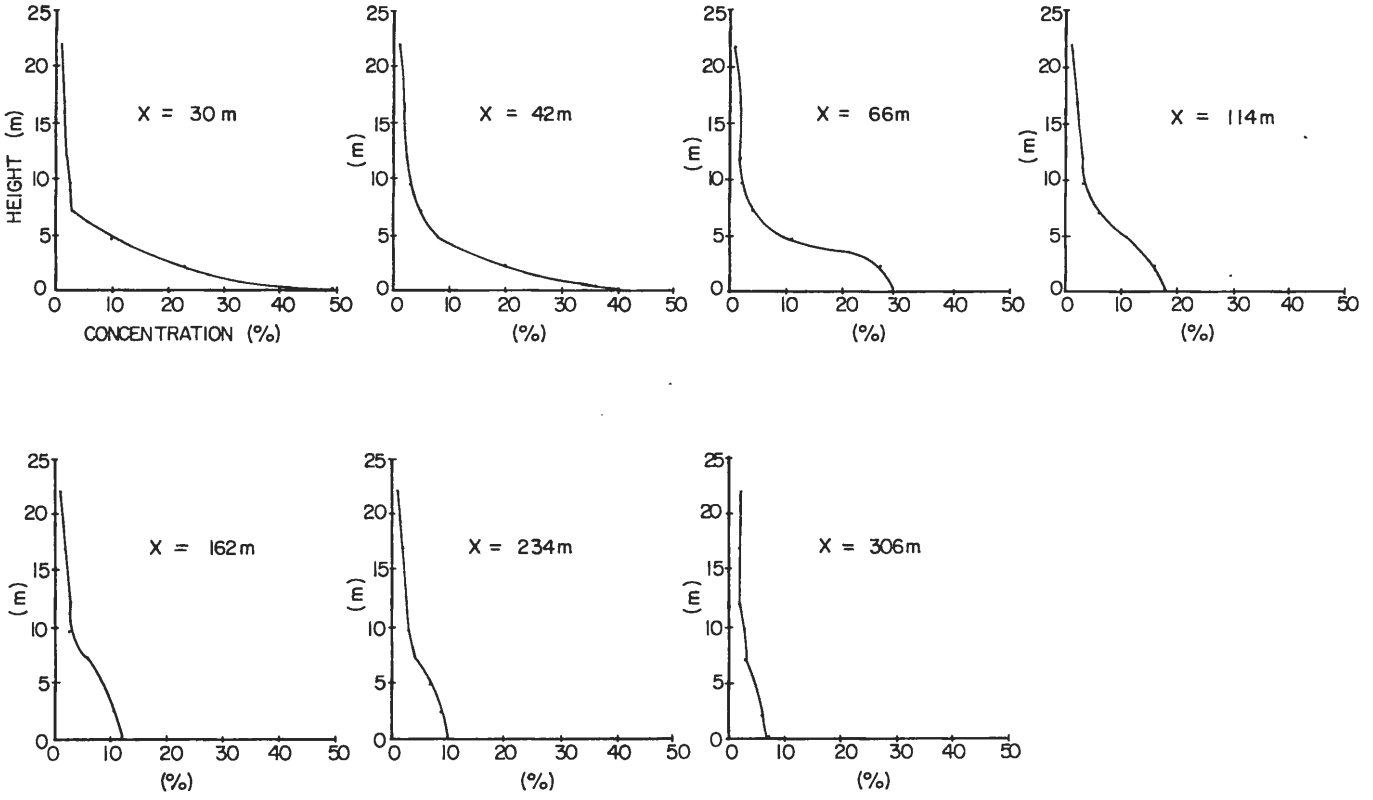

Figure 15. Vertical Peak Concentration Profiles (Run No. 7)

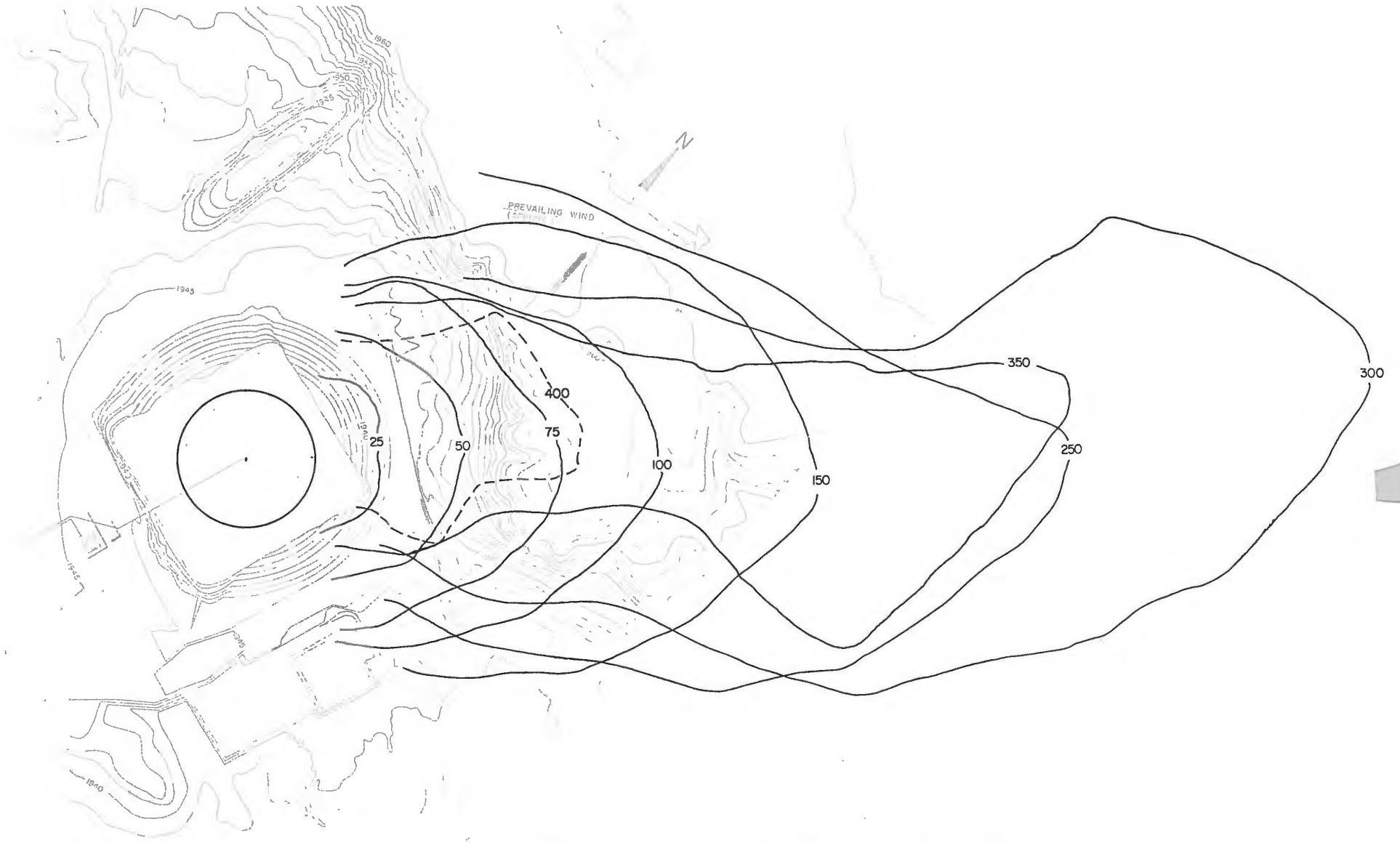

Figure 16-1. Time Progression of Ground Level LFL for Run No. 1 (all values in seconds)

Figure 16-2. Time Progression of Ground Level LFL for Run No. 2 (all values in seconds)

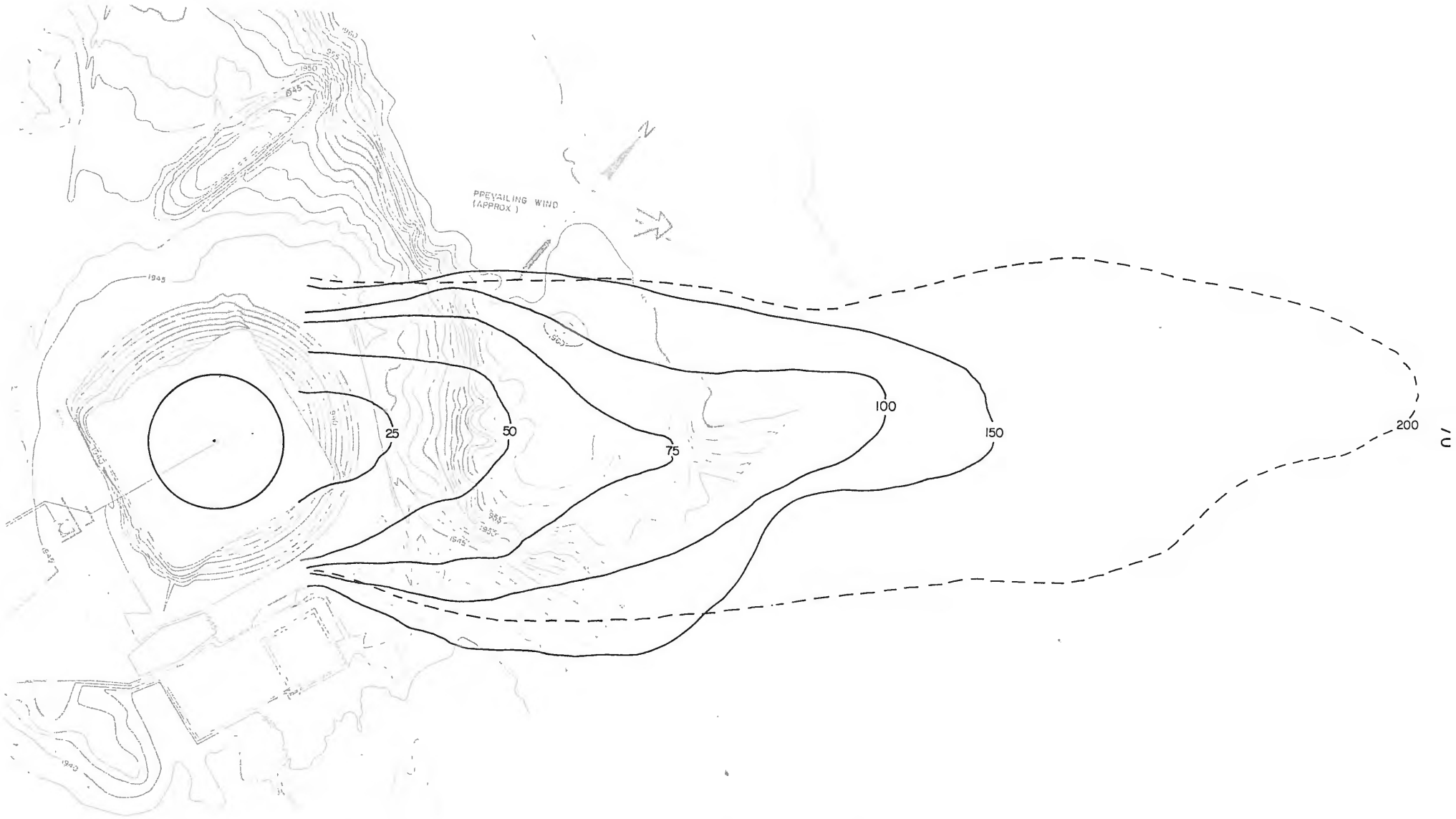

Figure 16-3. Time Progression of Ground Level LFL for Run No. 3 (all values in seconds)

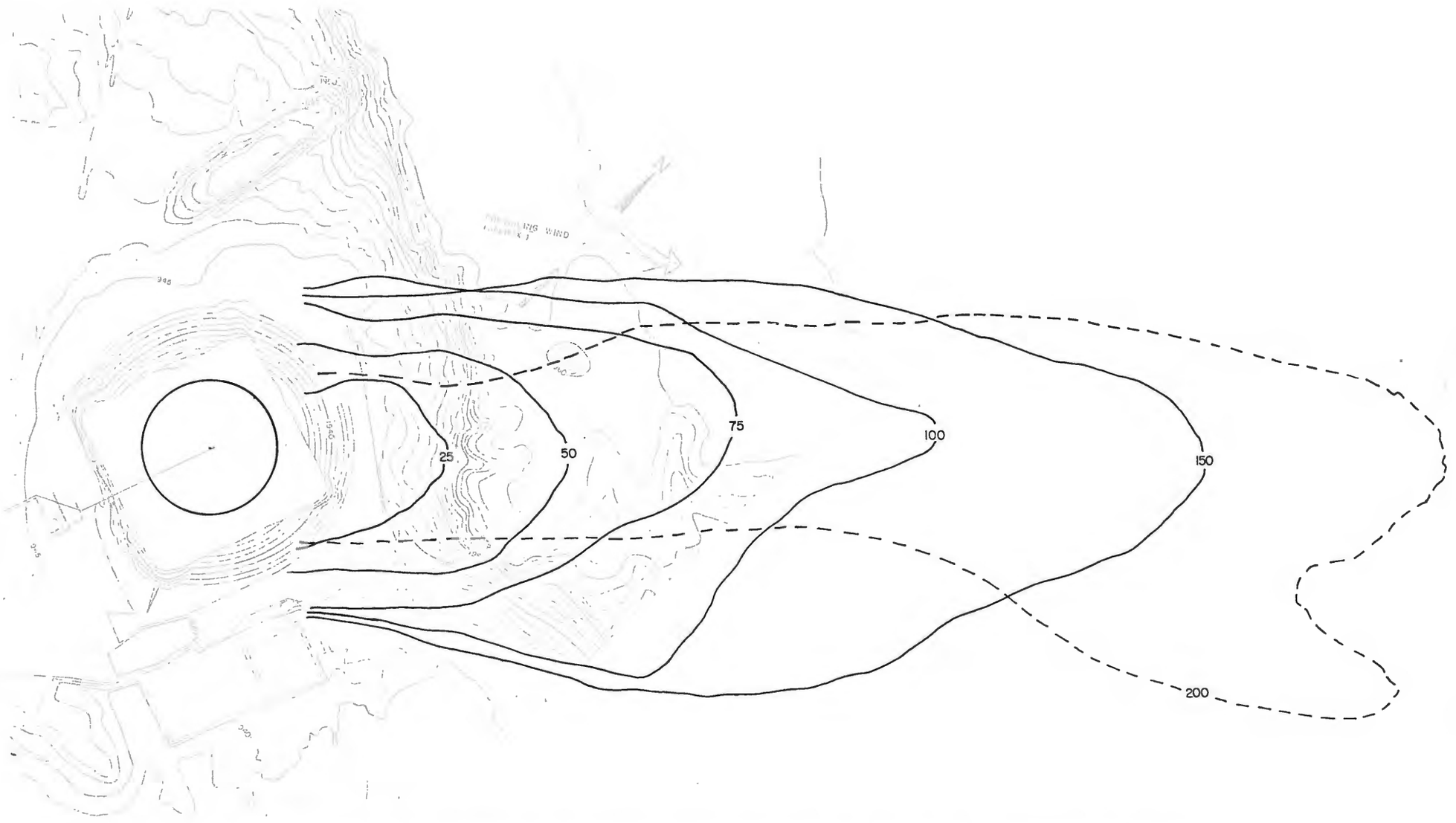

Figure 16-4. Time Progression of Ground Level LFL for Run No. 4 (all values in seconds)

Figure 16-5. Time Progression of Ground Level LFL for Run No. 5 (all values in seconds)

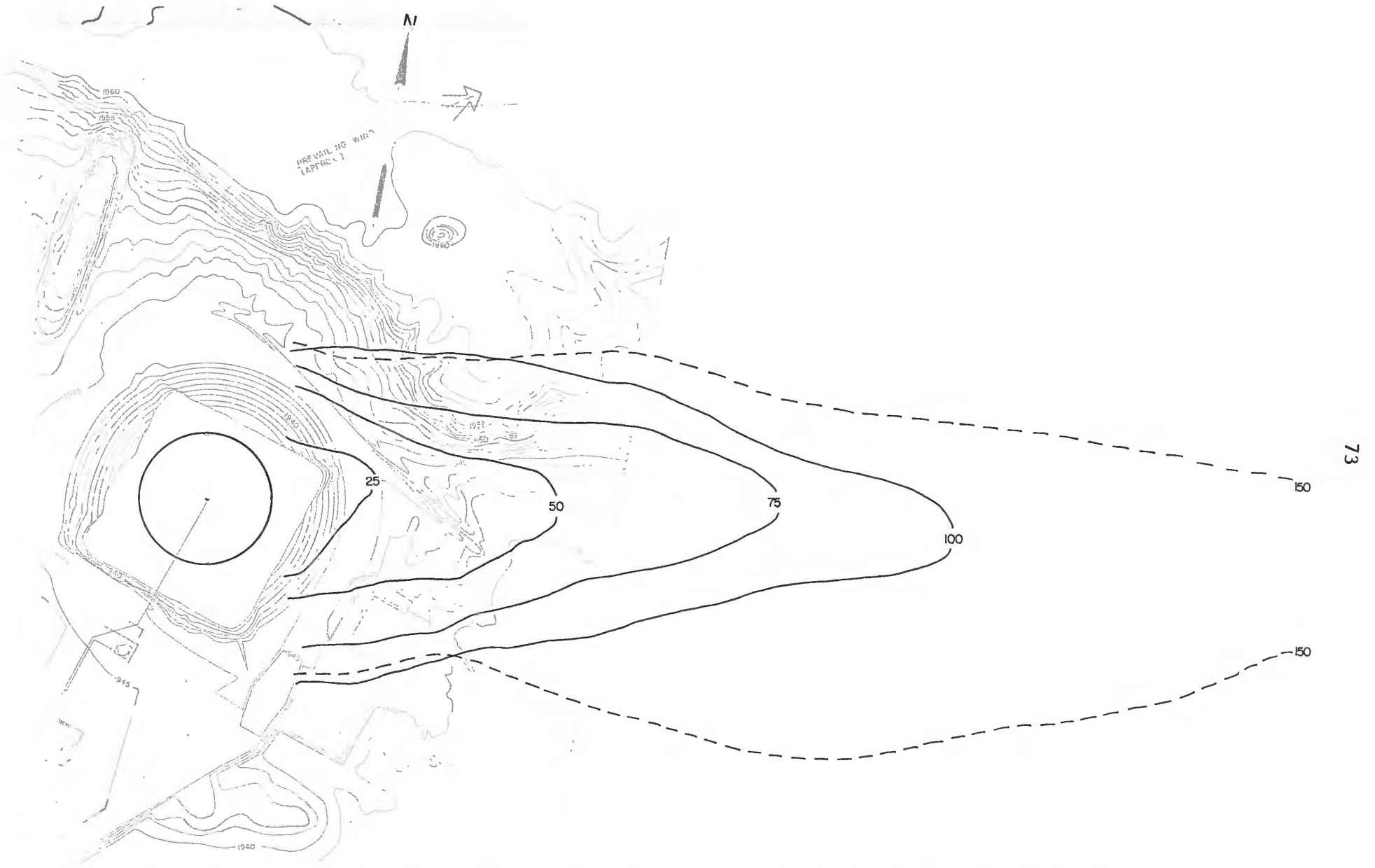

Figure 16-6. Time Progression of Ground Level LFL for Run No. 6 (all values in seconds)

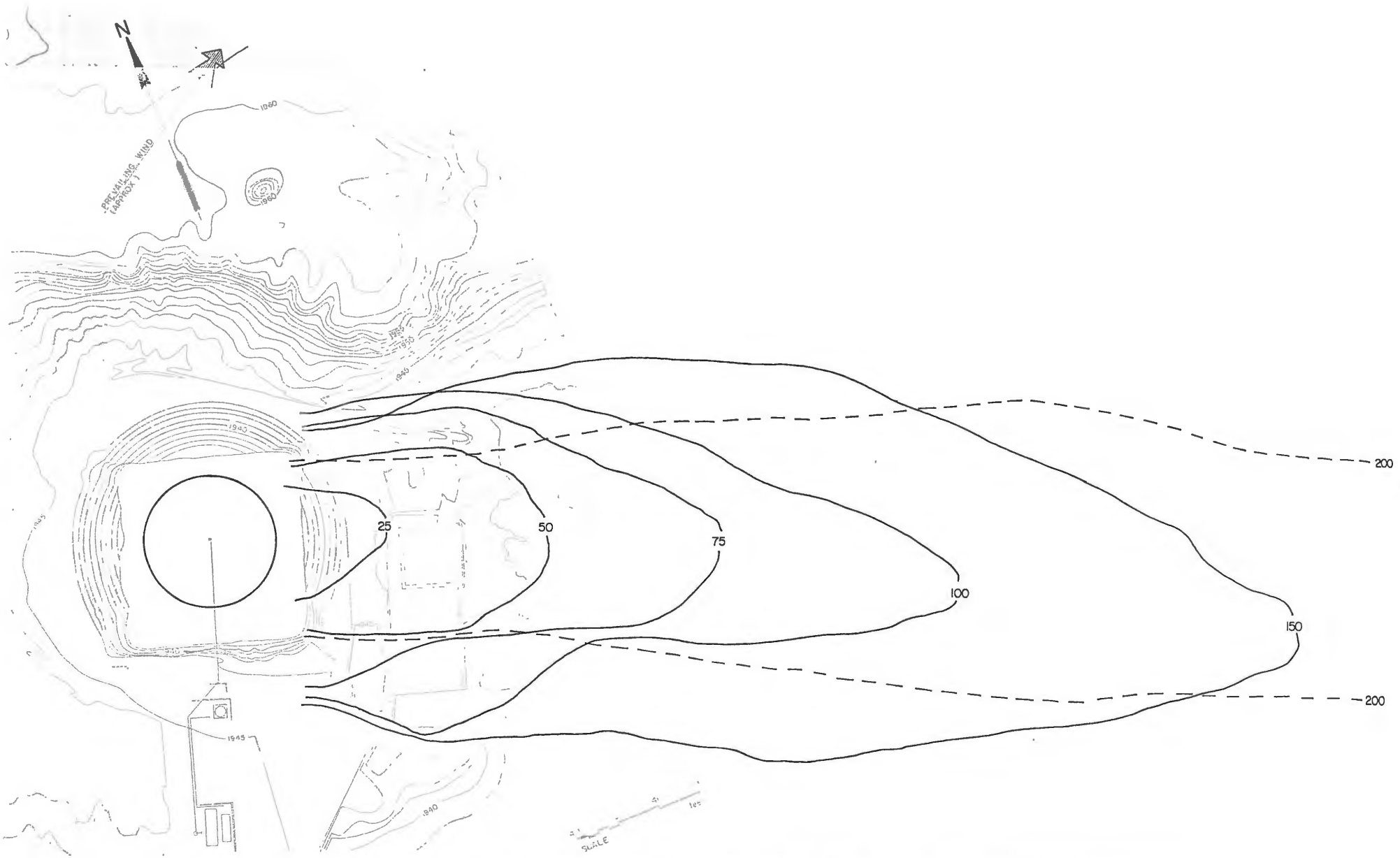

Figure 16-7. Time Progression of Ground Level LFL for Run No. 7 (all values in seconds)

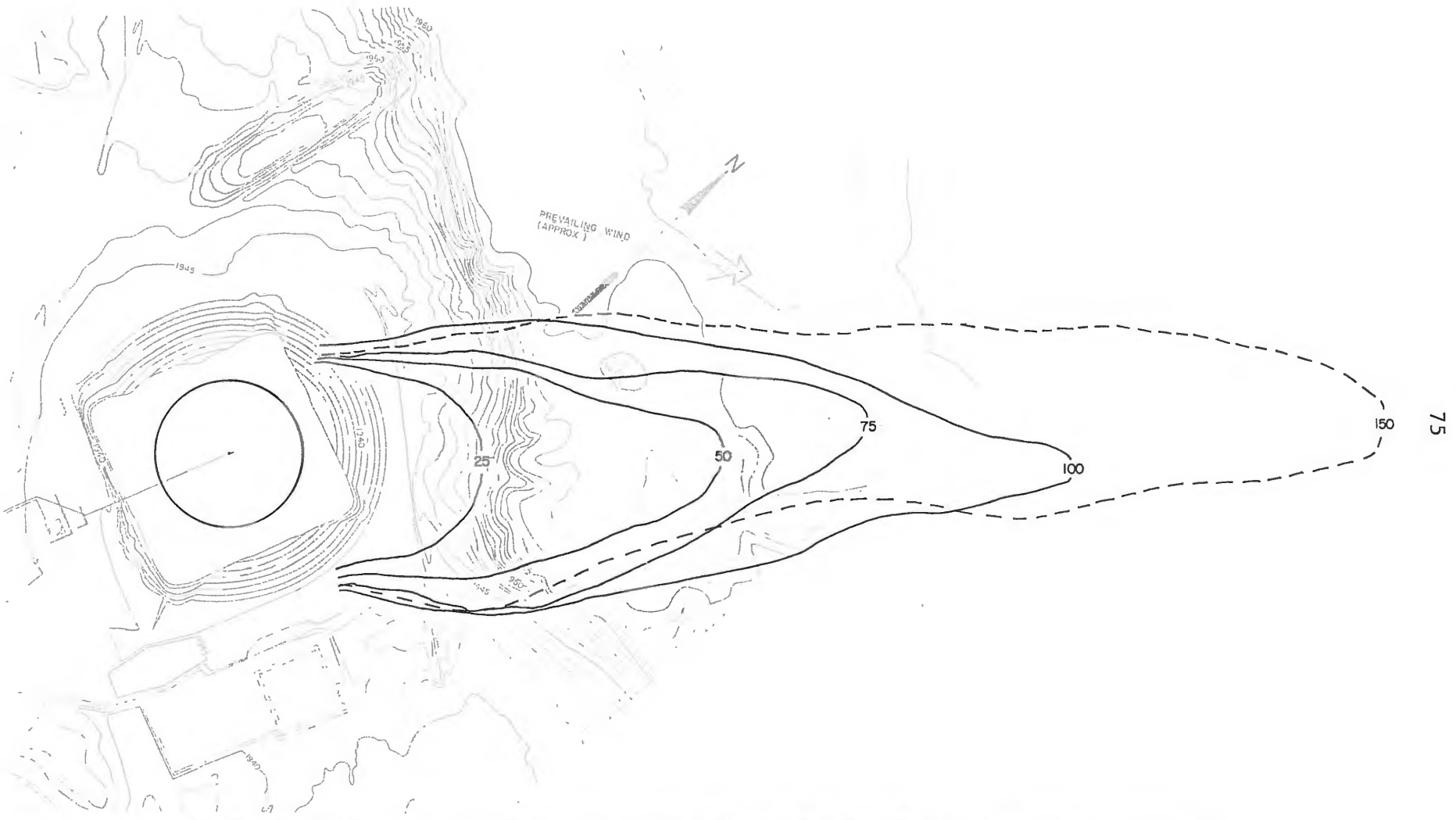

Figure 16-8. Time Progression of Ground Level LFL for Run No. 8 (all values in seconds)

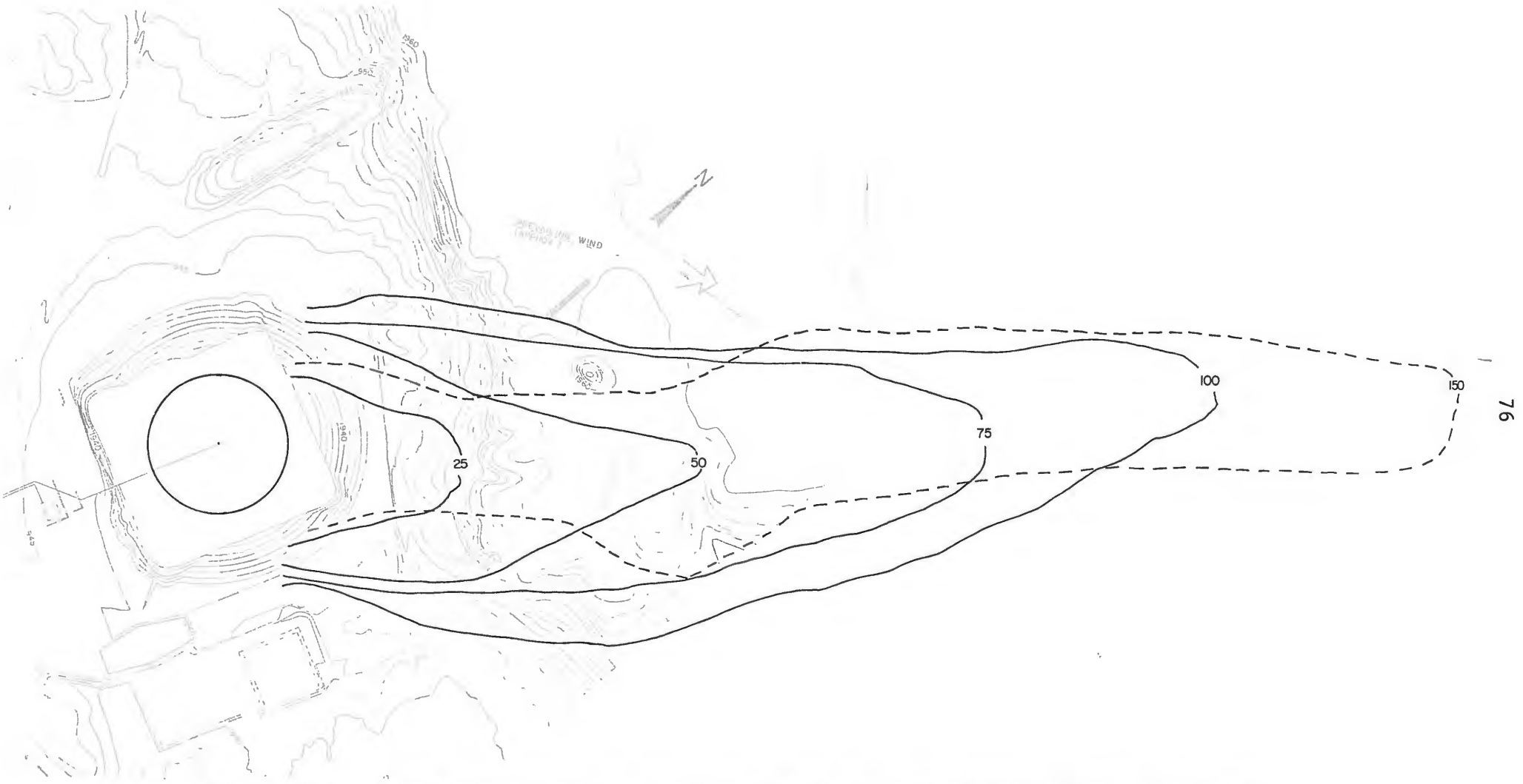

Figure 16-9. Time Progression of Ground Level LFL for Run No. 9 (all values in seconds)

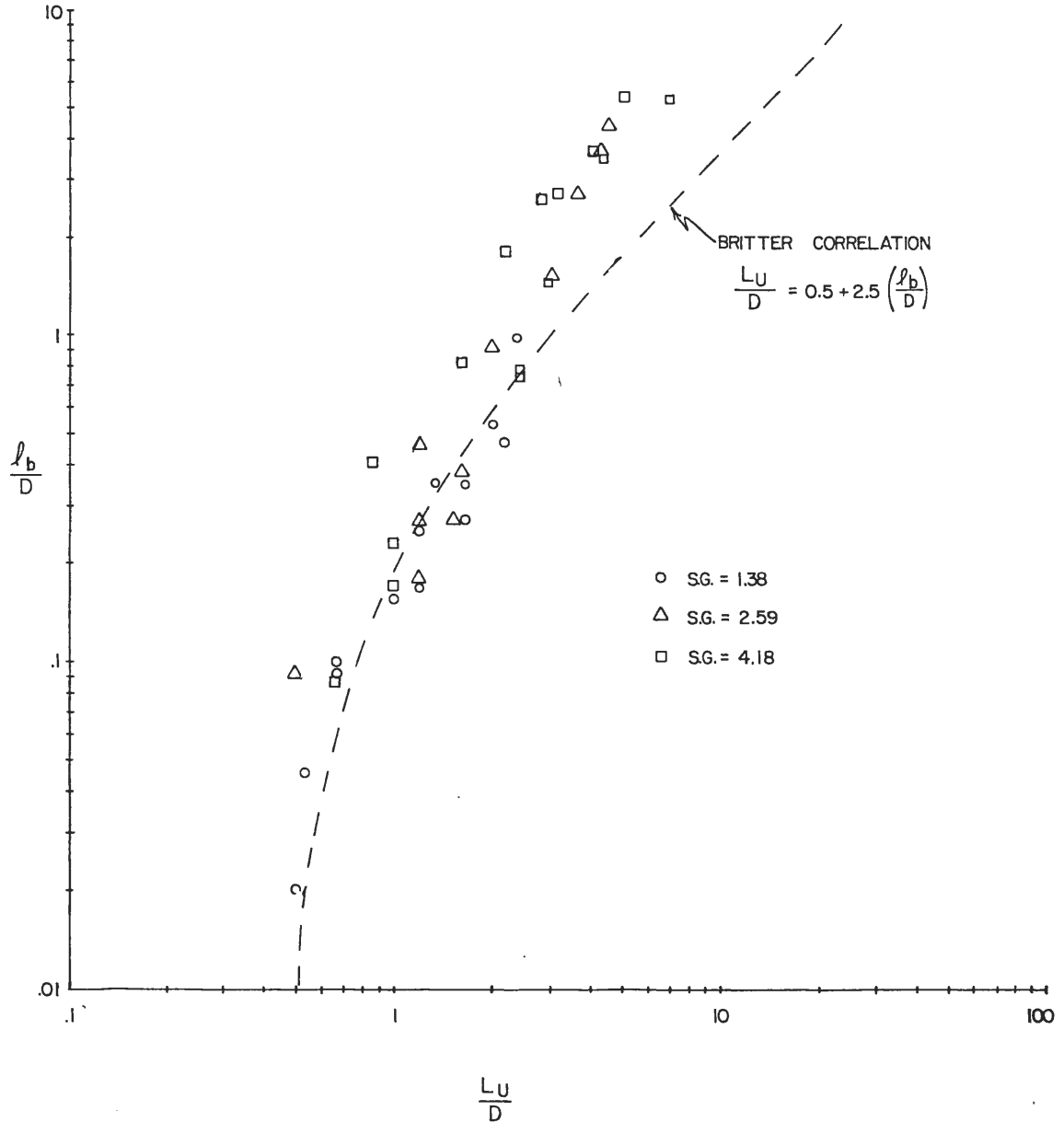

Figure 17. Buoyancy Length Scale vs. Upstream Travel Distance of Plumes

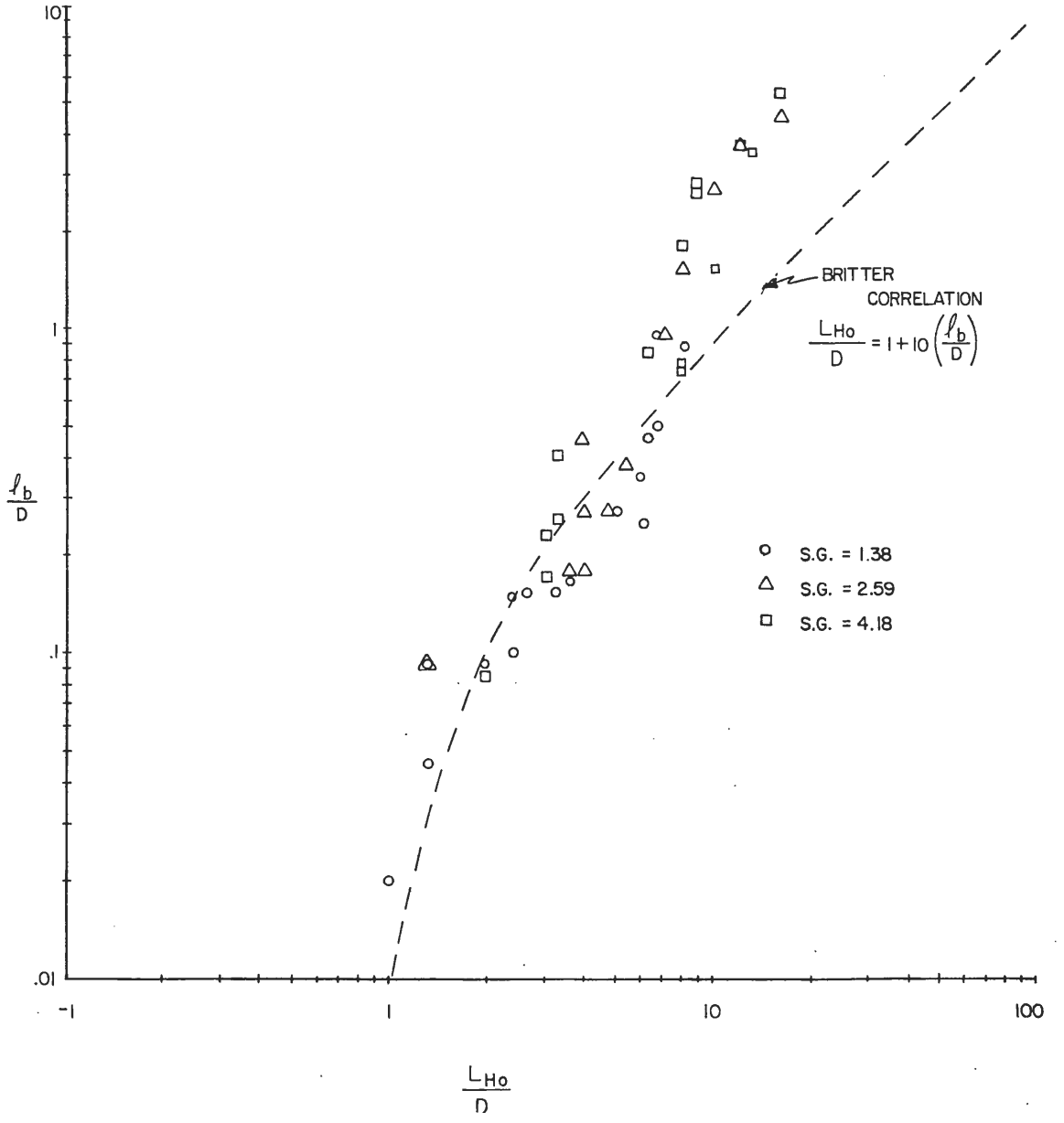

Figure 18. Buoyancy Length Scale vs. Lateral Travel Distance of Plume

APPENDIX A - THE CALCULATION OF MODEL SCALE FACTORS

As discussed previously in Section 2.3 the dominant scaling criteria for the simulation of LNG vapor cloud physics are the Froude number and the volume flux ratio. By setting these parameters equal for model and prototype one obtains the following relationships for a model (length scale (L.S.) of 1:240 and a model specific gravity (S.G.) of 1:38)

$$(U_a)_m = \left(\frac{S.G._m - 1}{S.G._p - 1}\right)^{0.5} \left(\frac{1}{L.S.}\right)^{0.5} (U_a)_p = 0.054\ (U_a)_p$$

$$Q_m = \left(\frac{S.G._m - 1}{S.G._p - 1}\right)^{0.5} \left(\frac{1}{L.S.}\right)^{2.5} Q_p = (1.12 \times 10^{-6})\ Q_p$$

$$t_m = \left(\frac{S.G._p - 1}{S.G._m - 1}\right)^{0.5} \left(\frac{1}{L.S.}\right)^{0.5} t_p = (0.078)\ t_p$$

$$L_m = \left(\frac{1}{L.S.}\right) L_p = (0.0042)\ L_p$$

In addition to these scaling parameters which govern the flow physics one must also scale the mole fractions (concentrations) measured in the model to those that would occur in the prototype. This scaling is required since the number of moles being released in a thermal plume are different from the number of moles being released in a isothermal plume. Hence, if corrected model concentration is n'_m then,

$$n_p = n'_m = (T_m/T_p)_{@\ b.o.}\ n_m\ ,\ n_p = n'_m = (2.70)\ n_m$$

By definition the concentration of LNG vapor is expressed as:

$$\chi_p = n_{NG}/(n_{NG} + n_a)$$

Substituting model equivalents into the above expression yields

$$\chi_p = \frac{(T_m/T_p)_{@b.o.} n_{Ar}}{(T_m/T_p)_{@b.o.} n_{Ar} + n_a} = \frac{n_{Ar}}{n_{Ar} + n_a (T_p/T_m)_{@b.o.}}$$

or

$$\chi_p = \frac{\chi_m}{\chi_m + (1 - \chi_m)(0.37)}$$

This equation was used to correct the modeled measurements to those that would be observed in the field.